AD-A154 042 SOME STUDIES IN FILTERING OF ATMOSPHERIC TURBULENCE(U) 1/1
NAVAL POSTGRADUATE SCHOOL MONTEREY CA C K LEE DEC 84

UNCLASSIFIED F/G 4/1 NL

END
FILMED
DTIC

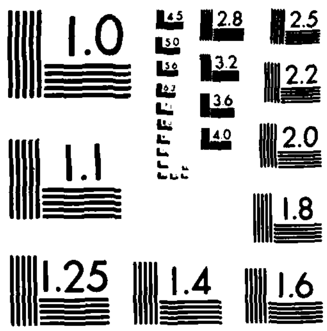

MICROCOPY RESOLUTION TEST CHART
NATIONAL BUREAU OF STANDARDS-1963-A

NAVAL POSTGRADUATE SCHOOL
Monterey, California

THESIS

SOME STUDIES IN FILTERING
OF
ATMOSPHERIC TURBULENCE

by

Cheong Koo Lee

December 1984

Thesis Advisor: J. V. Healey

SECURITY CLASSIFICATION OF THIS PAGE (When Data Entered)

REPORT DOCUMENTATION PAGE

READ INSTRUCTIONS BEFORE COMPLETING FORM

1. REPORT NUMBER / 2. GOVT ACCESSION NO. AD-A154042	3. RECIPIENT'S CATALOG NUMBER
4. TITLE (and Subtitle) Some Studies in Filtering of Atmospheric Turbulence	5. TYPE OF REPORT & PERIOD COVERED Master's Thesis; December 1984
	6. PERFORMING ORG. REPORT NUMBER
7. AUTHOR(s) Cheong Koo Lee	8. CONTRACT OR GRANT NUMBER(s)
9. PERFORMING ORGANIZATION NAME AND ADDRESS Naval Postgraduate School Monterey, California 93943	10. PROGRAM ELEMENT, PROJECT, TASK AREA & WORK UNIT NUMBERS
11. CONTROLLING OFFICE NAME AND ADDRESS Naval Postgraduate School Monterey, California 93943	12. REPORT DATE December 1984
	13. NUMBER OF PAGES 56
14. MONITORING AGENCY NAME & ADDRESS (if different from Controlling Office)	15. SECURITY CLASS. (of this report) Unclassified
	15a. DECLASSIFICATION/DOWNGRADING SCHEDULE

16. DISTRIBUTION STATEMENT (of this Report)

Approved for public release; distribution is unlimited.

17. DISTRIBUTION STATEMENT (of the abstract entered in Block 20, if different from Report)

18. SUPPLEMENTARY NOTES

19. KEY WORDS (Continue on reverse side if necessary and identify by block number)

Crossing Frequency; Filter; Atmospheric Turbulence; Spectral Density Function (von Karman, Kaimal, Teunissen)

20. ABSTRACT (Continue on reverse side if necessary and identify by block number)

This study, assuming stationary Gaussian turbulence model, investigates the effect on the crossing frequency of different spectral functions: von Karman, Kaimal and Teunissen for the x and z directions with five filters: ideal band-pass, ideal low-pass, "quadratic-type", "sine-type" and the Hanning. The filters have a much greater effect than the spectral functions. The estimated crossing frequency variation is as much as 50 percent among the quadratic-tyne, low-pass and sine-type filters. The Hanning filtering

predicts crossing rates up to thirty times, and the ideal one decade wide band-pass filtering predicts rates of eight times, higher than the ideal low-pass filtering. The variation, between the x and z direction, is less than 10 percent for the von Karman spectrum, and over 40 percent for the Teunissen one.

Approved for public release; distribution is unlimited.

Some Studies in Filtering of Atmospheric Turbulence

by

Cheong Koc Lee
Lieutenant Colonel, Republic of Korea Army
B.S., Korea Military Academy, 1972

Submitted in partial fulfillment of the
requirements for the degree of

MASTER OF SCIENCE IN ENGINEERING SCIENCE

from the

NAVAL POSTGRADUATE SCHOOL
December 1984

Author: ______________________
Cheong Koo Lee

Approved by: ______________________
James V. Healey, Thesis Advisor

____
Richard W. Bell, Second Reader

____
Max F. Platzer, Chairman,
Department of Aeronautics

____
John N. Dyer,
Dean of Science and Engineering

ABSTRACT

This study, assuming stationary Gaussian turbulence model, investigates the effect on the crossing frequency of different spectral functions: von Karman, Kaimal and Teunissen for the x and z directions with five filters: ideal band-pass, ideal low-pass, "quadratic-type", "sine-type" and the Hanning. The filters have a much greater effect than the spectral functions. The estimated crossing frequency variation is as much as 50 percent among the quadratic-type, low-pass and sine-type filters. The Hanning filtering predicts crossing rates up to thirty times, and the ideal one decade wide band-pass filtering predicts rates of eight times, higher than the ideal low-pass filtering. The variation, between the x and z direction, is less than 10 percent for the von Karman spectrum, and over 40 percent for the Teunissen one. keywords include:

TABLE OF CONTENTS

LIST OF TABLES

LIST OF FIGURES

ACKNOWLEDGEMENT

The author wishes to express his sincere appreciation to Professor James V. Healey, whose assistance and encouragement contributed immeasurably to this study. The author also wishes to dedicate this thesis to his wife, Yeongok. Without her constant support and understanding this work would not have been possible.

I. INTRODUCTION

Most flows occurring in nature and in engineering applications are turbulent. In the earth's boundary layer, differential heating of the atmosphere produces pressure gradients, which are subsequently modified by the rotation of the earth, causing a complex velocity field. In this boundary layer the wind speed decreases as the surface is approached due to both the frictional drag of the surface and the drag of all bodies protruding into the air flow. These retarding forces are transmitted through the layer by shear forces and by the exchange of momentum due to the vertical movement of the air. The process of momentum exchange between layers is the mechanism leads to the generation and decay of eddies which are termed turbulence. The resulting mixing of the air produces, along all three orthogonal axes, fluctuations in wind speed, commonly called gusts, which vary in size in both time and space.

The effects of this atmospheric turbulence has been of continuing concern to the aircraft or structure designer. Typical turbulence related problems are: the effects of turbulence on the fatigue life of the structure; the performance of control systems in turbulence and the determination of ultimate structural strength required to accept unsteady loads induced by turbulence. In an attempt to solve these problems, a number of statistical models of turbulence, which endeavour to describe the turbulence in terms of as few parameters as possible, have been proposed since early in this century. To analyze these problems, one needs to know the crossing frequency, which is the frequency with which a random function(here the filtered wind speed) crosses a prescribed value defined by a certain averaging time, say the hourly mean.

The crossing frequency depends largely on whether or not the random function is filtered, the type of filter and to a lesser extent,the spectral density function. The effects of type of filter used and spectral density expression will be discussed in detail later. The spectral density functions have been proposed by Dryden [Ref. 1], von Karman [Ref. 2], Kaimal [Ref. 3] and Teunissen [Ref. 4]. The Dryden expression makes mathematical analysis simple but is much less accurate than the others. The von Karman spectral function was recommended by the Engineering Sciences Data Unit (E.S.D.U.) [Ref. 5] and this expressions was originally postulated for isotropic turbulence. The effect of departure from isotropic turbulence near the ground is allowed for by the variation with height and surface roughness of the appropriate variance σ and length scale parameter L_i since they typify the intensity and size of eddies constituting turbulence. The Kaimal expression, which is frequently used, was obtained recently for the surface layer over flat, uniform, relatively featureless terrain in Kansas. The Teunissen model, which is a modified Kaimal one, was obtained for the generally rougher gross features of the upstream terrain.

In the following discussion, we will review turbulence models and spectral density functions. The spectral density S(n), in non-dimensional form, is a function of the dimensionless parameter nL_i/U, where n is frequency and L_i is the length scale of the turbulence and U is the mean hourly wind speed. E.S.D.U. [Ref. 5] gives empirical expressions for the length scale obtained by analysing its collection of world-wide turbulence data. Finally, for given values of nL_i/U, we will estimate the crossing frequencies with von Karman, Kaimal and Teunissen spectral expressions.

II. TURBULENCE MODELS

A. DISCRETE GUSTS MODEL

Powell and Connell [Ref. 6] defined gusts as constituting any series of discrete velocity-time events that can be defined from a turbulence time series according to some extrinsic criterion. There are two fundamentally different treatments of gust time; one is that the gust time is arbitrarily fixed and the other is that the gust time varies. Examples of this latter type of gust definition, shown in Figure 2.1, represent a sample of wind fluctuation in the form of a wind-component time series.

The GUST0 and GUST1 models define gust events in terms of gust amplitudes and characteristic times. Definitions of amplitudes and times differ for the two models. The GUST0 model can be completely specified in terms of a positive peak amplitude $+A_0$, and the time interval $+T_0$ between zero crossings on either side. It can also be specified in terms of a negative peak amplitude $-A_0$ and the corresponding time interval $-T_0$. Both definitions are expected to yield similiar statistics. Powell and Connell combine both posi-\~e and negative values into one set for their analysis.

The GUST1 model can be specified in terms of a positive amplitude $+A_1$ which is the peak-to-peak amplitude between adjacent minima and maxima, and a time interval $+T_1$ between the minima and the maxima; the positive sign indicates a positive rate of change in the variable. A comparable definition can be made in terms of amplitude $-A_1$ and time $-T_1$, where the negative sign indicates a negative rate of change in the variable.

One can find the impulse function of Equation(4.9) by inverse Fourier transform, i.e.,

$$h_4(t) = \frac{1}{2\pi}\int_{-\infty}^{\infty}(n_c^2 + n^2)^{-1/2} e^{j2\pi nt}\, dn$$
$$= \frac{1}{2\pi}\int_{-\infty}^{\infty}(n_c^2 + n^2)^{-1/2} \cos 2\pi nt\, dn +$$
$$\frac{1}{2\pi}\int_{-\infty}^{\infty}(n_c^2 + n^2)^{-1/2} (j\sin 2\pi nt)\, dn \qquad (4.10)$$

The second term of above equaticn is zero, since, it is an odd function. Thus Equation(4.10) becomes

$$h_4(t) = \frac{1}{\pi}\int_{0}^{\infty}(n_c^2 + n^2)^{-1/2} \cos 2\pi nt\, dn$$

or

$$h_4(t) = \frac{1}{\pi} K_0 (n_c t) \qquad (4.11)$$

where K_0 is the modified Bessel function.

The functions $h_4(t)$ and F_4 (n) are shown in Figure 4.1 and Figure 4.2.

The cut-off frequencies are defined formally as the frequencies at which the filters reach the first zero. But, when a real filter is used, we must find some equivalent cut-off frequency, which is defined as the cut-off frequency of an equivalent ideal filter whose area is equal to that of the real filter. [Ref. 11] Greenway [Ref. 12] and Powell and Connell [Ref. 6] have used the value at the half-power (3db) point of the filter as the cut-off frequency. Vinnichenko et al. [Ref. 11] defined the equivalent cut-off frequency as

$$n_c = \int_{0}^{\infty}|F(n)|\, dn \,. \qquad (4.12)$$

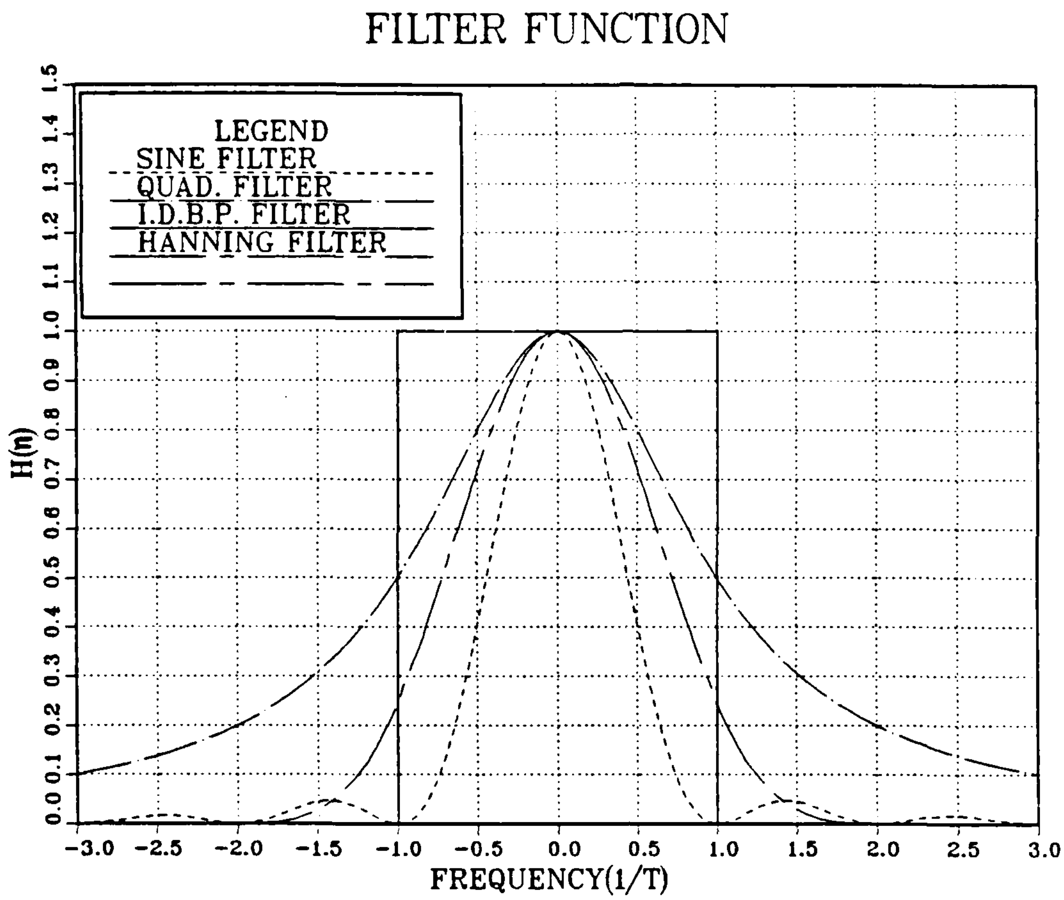

Figure 4.2 Filter Function $F_1(n)$, $F_2(n)$, $F_3(n)$ and $F_4(n)$.

The corresponding transfer function $F_3(n)$ has the form

$$F_3(n) = \left(\frac{\sin n\pi T n}{\pi T n}\right)^2 \frac{\pi^4}{[\pi^2 - (\pi T n)^2]^2} \qquad (4.8)$$

The advantage of $F_3(n)$ over $F_2(n)$, is that it has much smaller side maxima.

Another commonly used filter function is the quadratic filter function given by

$$F_4(n) = \frac{1}{n_c^2 + n^2} \qquad (4.9)$$

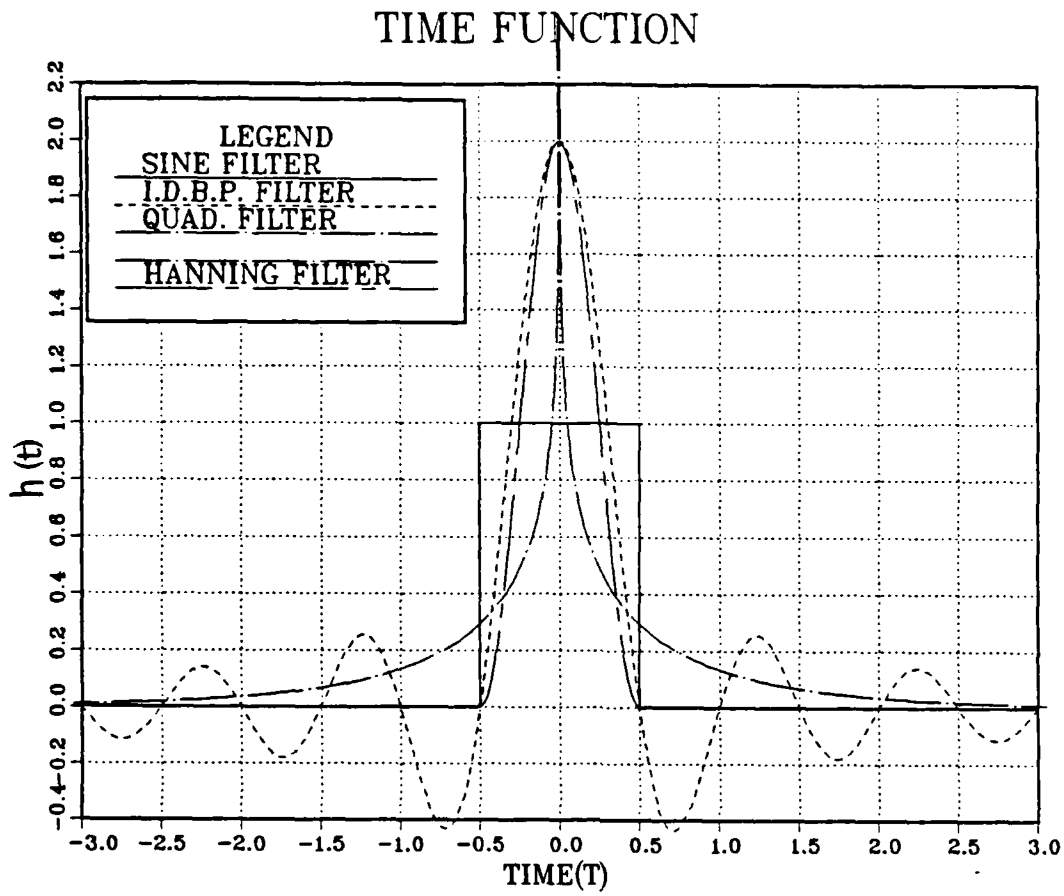

Figure 4.1 Time Function $h_1(t)$, $h_2(t)$, $h_3(t)$ and $h_4(t)$.

The function $h_2(t)$ and $F_2(n)$ are shown in Figure 4.1 and Figure 4.2 respectively. The figure shows that $F_2(n)$ is a low-frequency filter with cut-off frequency $n_c = 1/T$. The shape of this filter shows that frequencies above n_c are transmitted nonuniformly and those below n_c are completely suppressed.

The impulse response function $h_3(t)$, called the smoothed moving average is:

$$h_3(t) = \begin{cases} \dfrac{1+\cos(2\pi/T)t}{T} & \text{when } -T/2 \le t \le T/2 \\ 0 & \text{when } |t| > T/2 \end{cases} \qquad (4.7)$$

A. FILTER FUNCTIONS

It is clear that the quality of the crossing frequency estimates obtained by means of Equation (4.2) will depend strongly on the form of the filter function $F(n)$ and, hence, on the selection of the time function $h(t)$. Thus we will consider some examples of the function $h(t)$ and filter function $F(n)$ corresponding to them. Let the time function be given by

$$h_1(t) = \frac{2}{T} \frac{\sin(2\pi t/T)}{2\pi t/T} \tag{4.3}$$

If we take Fourier transform, the Equation (4.3) becomes

$$F_1(n) = \begin{cases} 1 & \text{when } |n| < 1/T \\ 1/2 & \text{when } |n| = 1/T \\ 0 & \text{when } |n| > 1/T. \end{cases} \tag{4.4}$$

Graphs of the functions $h_1(t)$ and $F_1(n)$ are shown in Figure 4.1 and Figure 4.2 respectively and they represent an ideal band-pass filter.

The simple impulse response function $h_2(t)$ is the ordinary moving average:

$$h_2(t) = \begin{cases} 1/T & \text{when } -T/2 \leq t \leq +T/2 \\ 0 & \text{when } |t| > T/2 \end{cases} \tag{4.5}$$

The corresponding filter function $F_2(n)$ $(F_2(n)=H_2(n)^2)$, where $H_2(n)$ is the Fourier transform of the function $h_2(t)$, has the form

$$F_2(n) = \left(\frac{\sin \pi T n}{\pi T n} \right)^2 \tag{4.6}$$

IV. CROSSING FREQUENCIES

The instantaneous horizontal wind speed is considered to be composed of a mean longitudinal component U plus fluctuating component v_i, where the subscript i designates the x, y, or z component in a coordinate system with x oriented along the mean wind vector and z upwards. Then the wind speed as a function of time is given by

$$V(t) = U + v_i(t) \tag{4.1}$$

The average frequency of positive-slope level crossing N_{oi}, with which the wind speed fluctuations exceed their zero value, for a Gaussian distribution of turbulence, is given by

$$N_{oi} = \left[\int_{n_{c1}}^{n_{c2}} n^2 F(n) S_i(n)\,dn \Big/ \int_{n_{c1}}^{n_{c2}} F(n) S_i(n)\,dn \right]^{1/2} \tag{4.2}$$

where n_c is cut-off frequency, i is u,v,or w and F(n) is a filter function.

The value of N_{oi} depends on the mean wind speed U, L_i and turbulence intensity σ_i/U, which is a measure of the magnitude of turbulence fluctuations and defined as the ratio of the standard deviation of the instantaneous fluctuating velocity component to the mean wind speed averaged over arbitrary time, usually hourly, and depends only on the height $\tilde{z}$ and the terrain roughness z_o, in a stable atmosphere.

function of the gust velocity can be found by integration, i.e.,

$$P = \int_{-\infty}^{i_p} p(i)\,di \qquad (3.9)$$

In practice, atmospheric turbulence contains patches of a significantly non-Gaussian nature (particularly in the lower 30m) when larger gusts and longer lulls may occur more frequently then indicated by the Gaussian distribution. Kaimal et al. [Ref. 10] observed that the assumption of a stationary Gaussian process has validity only for the filtered data, not for the unfiltered time series.

where $f=nL_i/U$ and u_* is friction velocity. These expressions were derived from the data which were obtained from a horizontal array of tower-mounted propeller anemometers (z=11m) during a five-hour period for which the mean wind direction was virtually perpendicular to the main span of the array, in the city of Toronto, Canada.

As for the reason for the higher spectral energies found by Teunissen in the low-frequency region of the spectra in comparison with the Kaimal values which was measured in Kansas, this is not entirely obvious, apart from the rougher terrain for Teunissen experiment. Teunissen has suggested that the power spectra over a wide range of terrain types may possibly be represented by using above expressions with appropriate values of such 'terrain scaling' parameters.

B. PROBABILITY DENSITY

In general, a knowledge of the spectral density of a random process does not enable us to determine its probability density or distribution. However, a common assumption which is reasonable in many applications is that atmospheric turbulence is a 'normal' or Gaussian process, as discussed above, with a probability density function for which

$$p(i)=\frac{1}{\sigma_i\sqrt{2\pi}}\exp\left[-i^2/2\sigma_i^2\right] \tag{3.8}$$

where i=u(t), v(t) or w(t) are wind-speed fluctuations, which have a zero mean. Note that Equation (3.8) depends only on the standard deviation of the gust velocity. Thus, if the probability distribution of σ is known, the distribution

Another commonly used spectral expression is the Kaimal one; [Ref. 3]

$$\frac{nS_i(n)}{\sigma_i^2} = \frac{0.164(f/f_o)}{1+0.164(f/f_o)^{5/3}} \tag{3.4}$$

where $nS(n)$ = logarithmic power spectral density

σ_i^2 = variance of i

f = reduced frequency

f_o = reduced frequency at the intercept of the extrapolated inertial subrange slope with the $nS_i(n)/\sigma_i^2=1$ line; or in our notation, $f_{oi}=0.041z/L_i$.

The Kaimal expression is more common in the meteorological literature and was obtained as a best-fit to surface-layer measurements over uniform, flat, relatively featureless terrain.

Teunissen [Ref. 4] observed that von Karman model appears to be somewhat better than the Kaimal model at low frequencies. The Kaimal model largely underestimates the spectral content at these frequencies for all components(x,y,and z). On the other hand, the Kaimal model shape appears to be better than that of the von Karman model.

Teunissen has proposed modified Kaimal spectral expressions, given by

$$\frac{nS_u(n)}{u_*^2} = \frac{105f}{(0.44+33f)^{5/3}} \tag{3.5}$$

$$\frac{nS_v(n)}{u_*^2} = \frac{17f}{(0.38+9.5f)^{5/3}} \tag{3.6}$$

$$\frac{nS_w(n)}{u_*^2} = \frac{2f}{0.44+5.3f^{5/3}} \tag{3.7}$$

Spectral functions of atmospheric turbulence provide information on the frequency distribution of the kinetic energy of the various fluctuating velocity components. Used in conjunction with certain transfer functions, they provide information about the dynamic loading on, and response of, building and aircraft structures in the atmospheric wind.

A considerable number of measurements of the power spectra of gust velocities in the near-neutral atmosphere, or strong wind conditions, at varying heights and for different terrains are available. The von Karman spectral expressions, which were exclusively used by E.S.D.U. [Ref. 5], for each velocity component(x, y and z direction) are given by

$$\frac{nS_u(n)}{\sigma_u^2} = \frac{4\tilde{n}_u}{(1+70.8\tilde{n}_u^2)^{5/6}} \tag{3.1}$$

$$\frac{nS_v(n)}{\sigma_v^2} = \frac{4\tilde{n}_v(1+755.2\tilde{n}_v^2)}{(1+283.2\tilde{n}_v^2)^{11/6}} \tag{3.2}$$

$$\frac{nS_w(n)}{\sigma_w^2} = \frac{4\tilde{n}_w(1+755.2\tilde{n}_w^2)}{(1+283.2\tilde{n}_w^2)^{11/6}} \tag{3.3}$$

where $\tilde{n}_u = L_u n/U$, $\tilde{n}_v = L_v n/U$, $\tilde{n}_w = L_w n/U$ and L_i is integral length scale which is a function only of the terrain roughness and height above ground for the x and y directions; for the z direction it is a function of elevation only. σ_i^2 is the variance of the wind velocity fluctuations about the hourly mean. These equations are in common use in the engineering literature and have the advantage that the integral length scale L_i are treated as 'free' scaling parameters which are chosen to match the estimated scales for a particular height and terrain type, while maintaining constant spectral shape.

III. SPECTRAL DENSITY AND PROBABILITY DENSITY

A. SPECTRAL DENSITY

In the field of mechanical and electrical oscillations, a large number of phenomena are governed by equations of the form

$$m \frac{d^2y}{dt^2} + c \frac{dy}{dt} + ky = f(t)$$

where, m, c and k are constants; f(t) is a given forcing function and y(t) represents the response of the system as a function of the time t.

If the above time dependent force f(t) is periodic, it can be expressed in terms of a Fourier series; this series represents the sum of a large number of forces of different amplitudes and frequencies. All elastic bodies have natural frequencies, and if this force is applied to an elastic system, and the amplitudes of the components near a natural frequency are not very small, then this force will drive the body into resonance. The body will then go through a very large number of stress cycles in a short period of time, possibly leading to fatigue failure.

To have stationary properties, a random signal must be assumed to continue over an infinite time, and in such a case neither the real nor the imaginary part of the Fourier transform converges to a steady value. In this case, we use the spectral density function, which has no convergence difficulty and which is applicable to a whole class of similarly generated functions.

behave like exp(-x) rather than $\exp(-x^2)$, as predicted by the Gaussian distribution [Ref. 8]. Recently Reeves, et al. [Ref. 9] have discussed in great detail a non-Gaussian model. On the other hand, References(6) and (10) indicate that filtered wind speeds(particularly with a band-pass 5-50 Hz filter) is reasonably Gaussian in character. In the present work, the Gaussian model is used exclusively.

The statistical quantities of most frequent interest are the mean, variance, probability density, autocorrelation function, power spectral density and crossing frequency. The power spectral shapes usually assumed are those proposed by von Karman, Kaimal and Teunissen. The crossing frequency with these three spectral expressions will be studied in more detail later.

form characterized by three parameters, the gust velocity standard deviation (σ), the scale length (L), and the averaged speed (U).

3) Each of the three gusts components is a Gaussian process.

The assumptions of the Gaussian model make it possible to calculate the statistics of any structure response for each region of turbulence as functions of the parameters L and σ of that region. Thus, the assumptions of structure linearity and the Gaussian nature of turbulence permit their evaluation with a minimum of difficulty. These results will be dependent upon the assumed values of L and σ along with the characteristics of the structure dynamics.

The continuous model is used primarily to evaluate response statistics for selected conditions in continuous turbulence. For this application both the scale length and standard deviation of the turbulence as well as the structure characteristics are fixed at values representative of certain conditions which could reasonably be expected to occur in service.

The three assumptions made above need some reconsiderations. The first assumption stated that the turbulence is stationary and homogeneous and the dimensions of structures are much smaller than the scale lengths of the gusts components. These conditions are not always satisfied. The second assumption of the power spectral model is valid at low altitudes, but is not so certain at high altitudes, the problem made being more difficult by a lack of data at the latter altitudes. The third assumpticn stated that the turbulence is a Gaussian process. However, some experimental data indicate that the Gaussian turbulence model significantly underestimates the frequency of occurence of high gust velocities [Ref. 7]. Furthermore, peak gust velocity cumulative probabilities of exceedance observed in atmospheric turbulence

sufficient damping, that each encounter with one of these gusts results in a single significant response peaks.

This model is typically sed to estimate ultimate strength requirements, however, it is not a satisfactory one for all aspects of the design problem. For example, its application in areas such as structural fatigue, control system performance, or even extreme responses which involve lightly damped modes is highly questionable. In most instances turbulence does not occur as discrete gusts but as a continuous random disturbance. Furthermore, this model neglects most of the dynamic characteristics of the vehicle. Thus, although the necessity of evaluating the responses of a proposed structure to discrete gusts is still recognized as an important part of the design procedure, the use of the discrete model to calculate most response statistics has largely given way in recent years to the use of turbulence models which attempt to take both the dynamic characteristics of the structure and the continuous nature of turbulence into consideration. This is known as the continuous or power spectral model.

B. CONTINUOUS MODEL

The basic idea of continuous model is that atmospheric turbulence can be represented by a continuous stochastic process which acts as a disturbing influence on the structure. The principal assumptions for this model are

1) Each encounter of an structure with continuous atmospheric turbulence can be modeled as a deterministic linear system perturbed by three independent stationary stochastic processes, which represent the longitudinal, lateral and vertical gusts components.
2) The spectral density of each random process has a

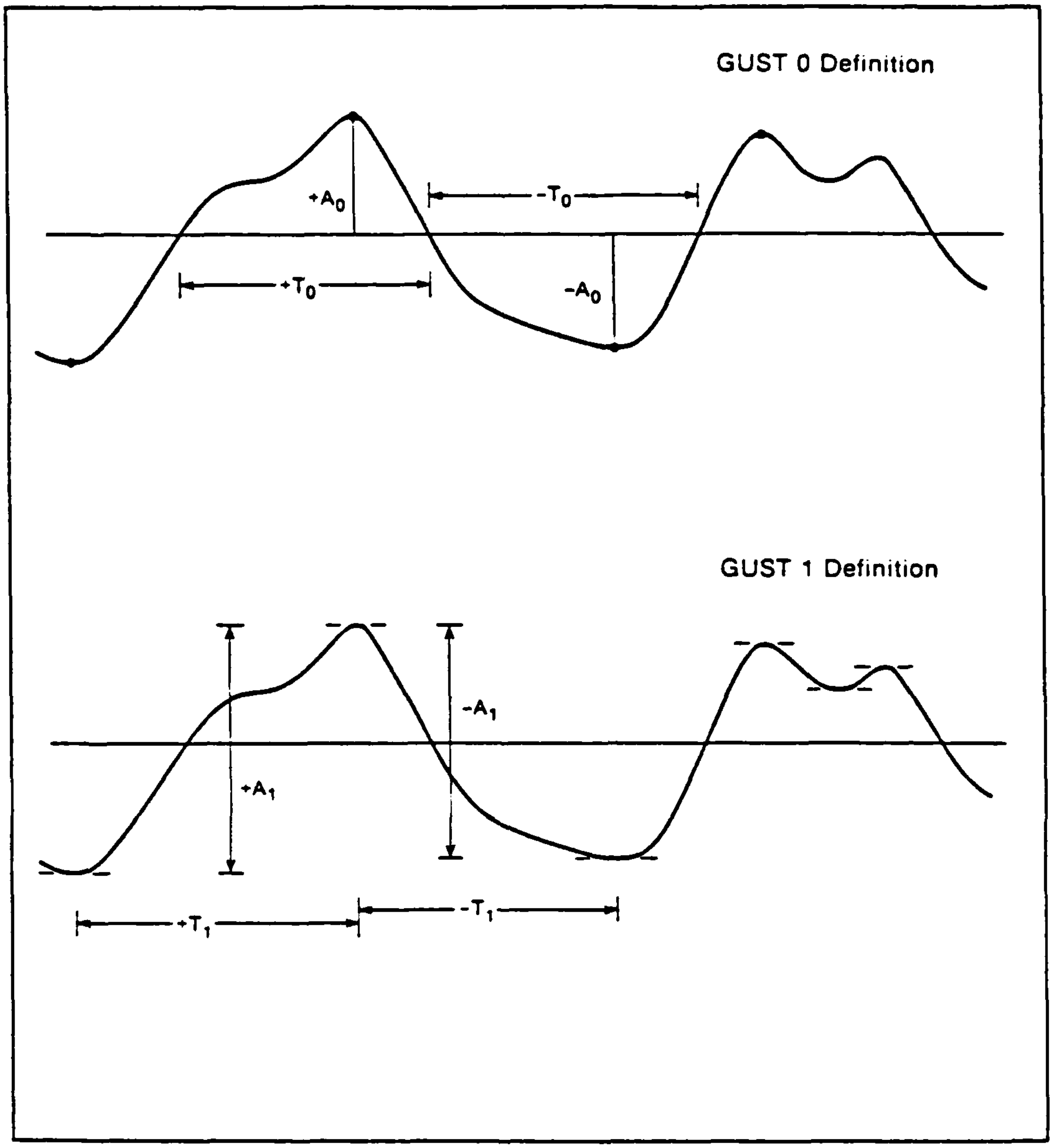

Figure 2.1 Definitions of GUST0 and GUST1.

The discrete model treats turbulence as a series of isolated gusts and the basic assumptions are

1) Atmospheric turbulence can be modeled as a collection of isolated gusts randomly distributed along the structure.
2) Gusts have random magnitude but fixed shape.
3) The structure is a deterministic linear system with

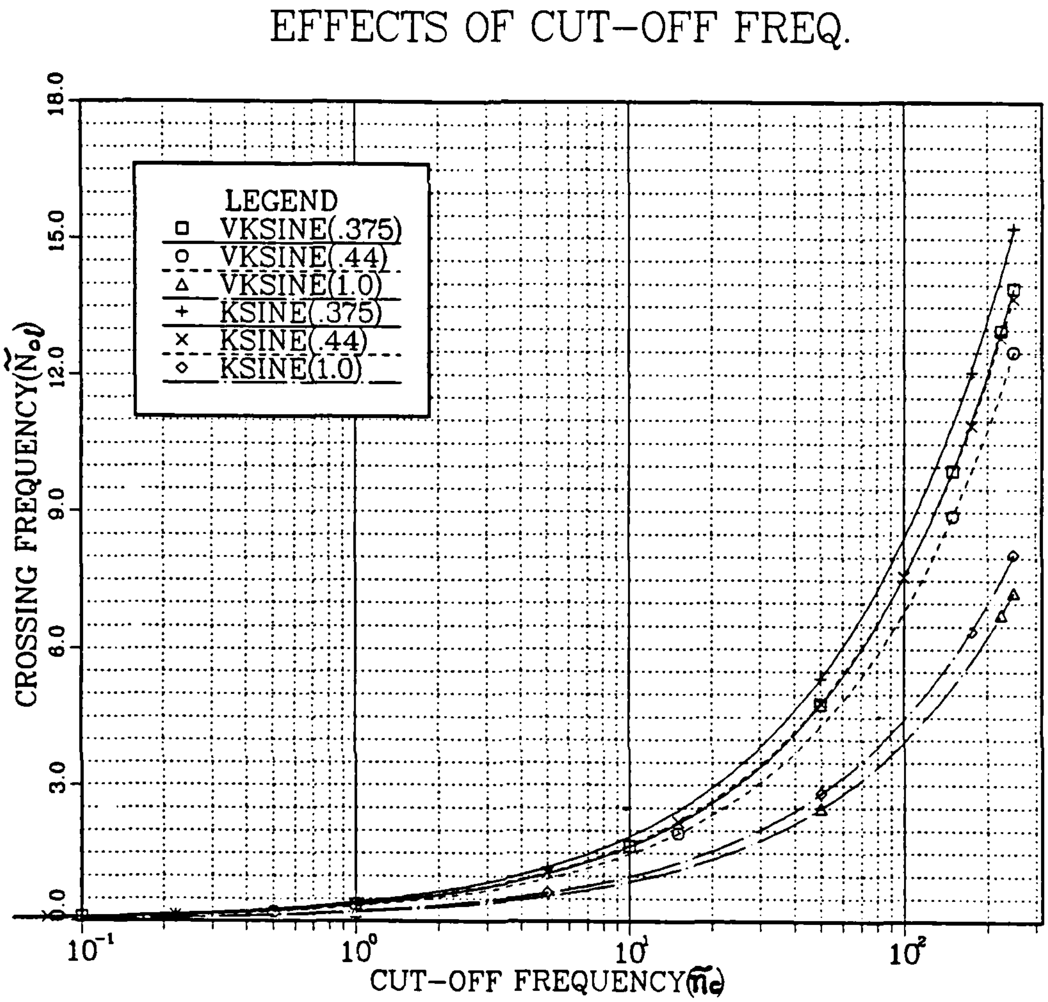

Figure 4.3 Effects of Cut-off Frequencies.

According to the Equation(4.12), the cut-off frequencies depend on the filtering function. The effects of cut-off frequency on the crossing frequencies are shown in Figure 4.3, which shows that the higher the cut-off frequency leads to lower zero crossing rates.

B. CALCULATION OF CROSSING FREQUENCIES

In this section the frequency of zero crossings are estimated using von Karman, Kaimal and Teunissen spectral density functions with various filter functions which we have discussed above.

1. Using the von Karman Spectral Density Function

Introducing the von Karman spectral density function for the x-direction $S_u(n)$ into Equation (4.2) yields

$$N_{ox} = \left[\int_{n_{c1}}^{n_{c2}} \frac{n^2 F(n)\,dn}{(1+70.8\tilde{n}_u^2)^{5/6}} \Big/ \int_{n_{c1}}^{n_{c2}} \frac{F(n)\,dn}{(1+70.8\tilde{n}_u^2)^{5/6}} \right]^{1/2} \qquad (4.13)$$

For numerical calculation, set $y=n/n_{c1}$ and $D=n_{c2}/10n_{c1}$ and Equation (4.13) transformed to

$$\tilde{N}_{ox} = \tilde{n}_{c1} \left[\int_{1}^{10D} \frac{y^2\,dy}{(1+70.8\tilde{n}_{c1}^2\, y^2)^{5/6}} \Big/ \int_{1}^{10D} \frac{dy}{(1+70.8\tilde{n}_{c1}^2\, y^2)^{5/6}} \right]^{1/2} \qquad (4.14)$$

where $\tilde{N}_{ox}$ is the dimensionless frequency of positive-slope level crossings for the x direction $N_{ox}L_u/U$. Equation (4.14) is for the ideal band-pass filter function of D decades filter width.

The upper integral of Eq. (4.13) will not converge as n_{c2} goes to infinity because the empirical expression for the turbulence spectrum employed does not account for the high-frequency range where viscous dissipation damps out turbulence fluctuations. One can achieve convergence by use of a suitable filter function. Introducing Equation (4.9) into Equation (4.13) yields

$$\tilde{N}_{ox} = \tilde{n}_c \left[\int_0^{\infty} \frac{y^2\,dy}{(1+70.8\tilde{n}_c^2 y^2)^{5/6}(1+y^2)} \Big/ \int_0^{\infty} \frac{dy}{(1+70.8\tilde{n}_c^2\, y^2)^{5/6}(1+y^2)} \right]^{1/2} \qquad (4.15)$$

If we take $F_2(n)$, here called the sine filter function, instead of quadratic filter, with the cut-off frequency $n_c=0.44/T$ which Greenway [Ref. 12] has used, and substitute into Equation (4.6), we find

$$F_2(n)=\sin^2(0.44\pi n/n_c)/(0.44\pi n/n_c)^2. \tag{4.16}$$

Introducing Equation (4.16) into Equation (4.13) and setting $y=0.44\pi n/n_c$ yields

$$\tilde{N}_{o\alpha}=\frac{\tilde{n}_c}{0.44\pi}\left\{\frac{\displaystyle\int_0^\infty \frac{\sin^2(y)\,dy}{\left[1+70.8(\tilde{n}_c/0.44\pi)^2 y^2\right]^{5/6}}}{\displaystyle\int_0^\infty \frac{[\sin^2(y)/y^2]\,dy}{\left[1+70.8(\tilde{n}_c/0.44\pi)^2 y^2\right]^{5/6}}}\right\}^{1/2} \tag{4.17}$$

If we use $F_3(n)$, which is the Hanning frequency window, and equate cut-off frequency $n_c=0.375/T$ as derived by Vinnichenko et al. [Ref. 11], then substitution into Equation (4.8) gives

$$F_3(n)=\left(\frac{\sin(0.375\pi n)}{0.375\pi n}\right)^2\frac{\pi^4}{\left[\pi^2-(0.375\pi n)^2\right]^2} \tag{4.18}$$

Substituting Equation (4.18) into Equation (4.13) and setting $y=0.375\pi n/n_c$ and $\tilde{\eta}_c=\tilde{n}_c/0.375\pi$ yields

$$\tilde{N}_{o\alpha}=\tilde{\eta}_c\left\{\frac{\displaystyle\int_0^\infty \frac{\sin^2(y)\,dy}{(1+70.8\,\tilde{\eta}_c^2\,y^2)^{5/6}\,(\pi^2-y^2)^2}}{\displaystyle\int_0^\infty \frac{[\sin^2(y)/y^2]\,dy}{(1+70.8\,\tilde{\eta}_c^2\,y^2)^{5/6}\,(\pi^2-y^2)^2}}\right\}^{1/2} \tag{4.19}$$

TABLE I

Crossing Frequencies (von Karman x-direction)

$\tilde{n}_c$	IDBP	QUAD	SINE	HANNING
0.100	0.3972	0.1215	0.0865	17.4480
0.125	0.4838	0.1116	0.0955	21.8074
0.150	0.5709	0.1250	0.1117	26.1670
0.175	0.6585	0.1381	0.1232	30.5267
0.220	0.8172	0.1604	0.1424	38.3741
0.500	1.8193	0.2737	0.2391	87.2049
1.000	3.6235	0.4298	0.3699	174.4062
2.000	7.2394	0.6765	0.5744	348.8093
5.000	18.0931	1.2365	1.0383	872.0234
10.000	36.1847	1.9555	1.6267	1744.0481
15.000	54.2766	2.5585	2.1230	2616.0669
22.000	79.6055	3.2989	2.7307	3836.9021
50.000	180.9212	5.6928	4.6950	8720.2461
75.000	271.3816	7.4555	6.1414	---
100.000	361.8425	9.0288	7.4326	---
150.000	542.7637	11.8268	9.7292	---
175.000	633.2241	13.1054	10.7787	---
200.000	723.6853	14.3243	11.7794	---
225.000	814.1465	11.4933	12.9392	---
250.000	904.6067	16.6196	13.6641	---

$\tilde{n}_c$=cut-off frequency
IDBP=ideal band-pass filter
QUAD="quadratic-type" filter
SINE="sine-type" filter
HANNING=HANNING filter
IDLP=ideal low-pass filter

The results of numerical calculations of Eqs.(4.14), (4.15), (4.17) and (4.19) are given in table I. The plots for above equations are shown in Figure 4.4. The plots showing how well these crossing frequencies co-incide depend on the length scale, mean wind speed and filter functions.

The von Karman spectral density function for the z-direction is given by Equation(3.3). The equation of the crossing frequency for the ideal band-pass filter function can be obtained by substituting Equation(3.3) into Equation(4.2) and is given by

$$\tilde{N}_{ox} = \tilde{n}_{c1} \left[\frac{\displaystyle\int_1^{10D} \frac{(1+755.2\tilde{n}_{c1}^2\, y^2)\, y^2\, dy}{(1+283.2\tilde{n}_{c1}^2\, y^2)^{11/6}}}{\displaystyle\int_1^{10D} \frac{(1+755.2\tilde{n}_{c1}^2\, y^2)\, dy}{(1+283.2\tilde{n}_{c1}^2\, y^2)^{11/6}}} \right]^{1/2} \tag{4.20}$$

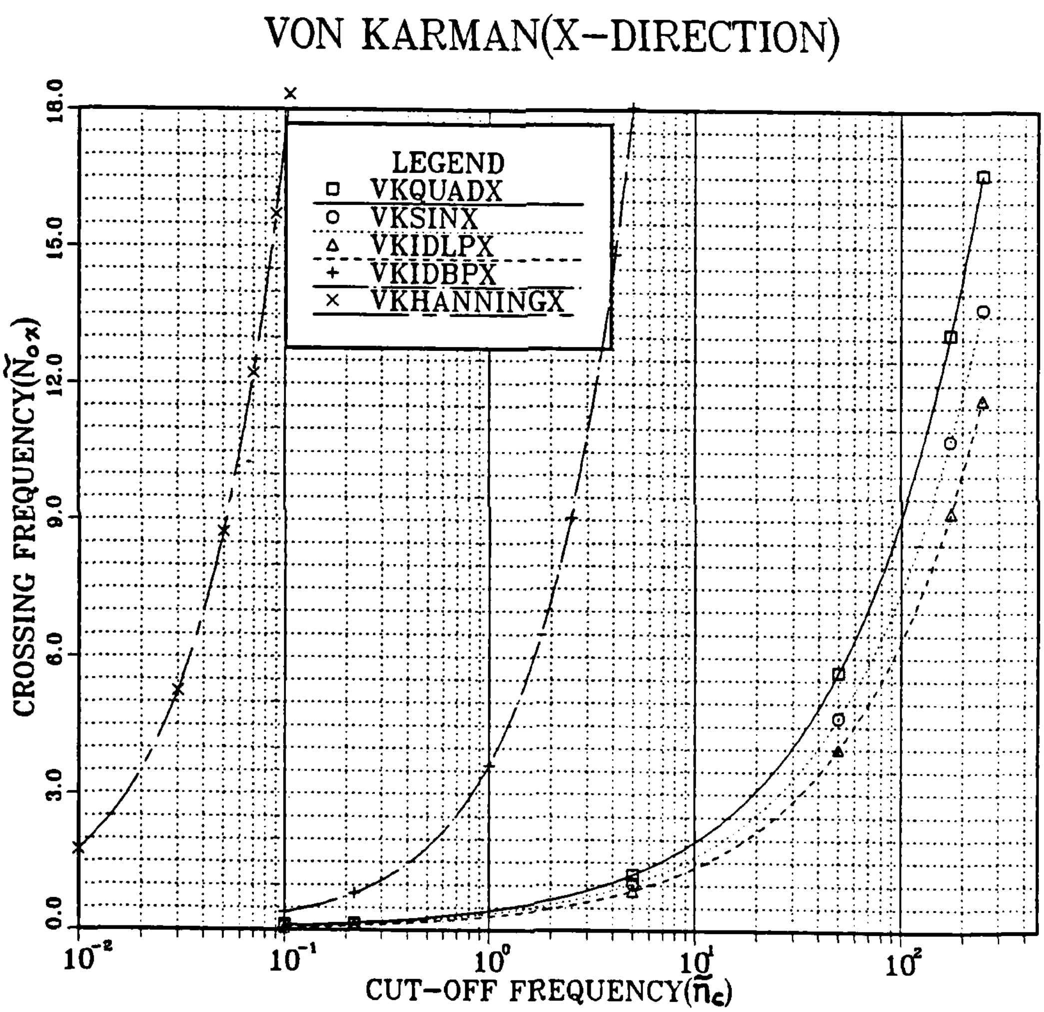

Figure 4.4 Crossing Frequencies with von Karman Spectral Expression for the x-direction.

Using the same procedure as for the x-direction, the z-direction crossing frequency for the quadratic filter function is found to be

$$\tilde{N}_{oz} = \tilde{n}_c \left[\frac{\displaystyle\int_0^\infty \frac{(1+755.2\tilde{n}_c^2 y^2)\, y^2\, dy}{(1+283.2\tilde{n}_c^2 y^2)^{11/6}(1+y^2)}}{\displaystyle\int_0^\infty \frac{(1+755.2\tilde{n}_c^2 y^2)\, dy}{(1+283.2\tilde{n}_c^2 y^2)^{11/6}(1+y^2)}} \right]^{1/2} \tag{4.21}$$

and, for the sine filter function, if one defines $\tilde{n}_c/0.44\pi = \tilde{\eta}_c$ the crossing frequency for the z-direction becomes

$$\tilde{N}_{oz} = \tilde{\eta}_c \left\{ \frac{\displaystyle\int_0^\infty \frac{[1+755.2(\tilde{\eta}_c y)^2]\sin^2(y)\, dy}{(1+283.2\tilde{\eta}_c^2 y^2)^{11/6}}}{\displaystyle\int_0^\infty \frac{[1+755.2(\tilde{\eta}_c y)^2][\sin^2(y)/y^2]\, dy}{(1+283.2\tilde{\eta}_c^2 y^2)^{11/6}}} \right\}^{1/2} \tag{4.22}$$

Introducing filter function F_3 (n) into Equation (4.20) and setting $y=0.375\pi n/n_c$ and $\tilde{n}_c/0.375\pi=\tilde{\eta}_c$ yields

$$\tilde{N}_{oz} = \tilde{\eta}_c \left\{ \frac{\displaystyle\int_0^\infty \frac{[1+755.2(\tilde{\eta}_c y)^2]\sin^2(y)\, dy}{(1+283.2\tilde{\eta}_c^2 y^2)^{11/6}(\pi^2-y^2)^2}}{\displaystyle\int_0^\infty \frac{[1+755.2(\tilde{\eta}_c^2 y^2)][\sin^2(y)/y^2]\, dy}{(1+283.2\tilde{\eta}_c^2 y^2)^{11/6}(\pi^2-y^2)^2}} \right\}^{1/2} \tag{4.23}$$

TABLE II

Crossing Frequencies(von Karman z-direction)

$\tilde{n}_c$	IDBP	QUAD	SINE	HANNING
0.100	0.3812	0.121	0.0816	17.4448
0.125	0.4686	0.136	0.0934	21.8044
0.150	0.5567	0.150	0.1044	26.1641
0.175	0.6454	0.163	0.1144	30.5238
0.220	0.8059	0.185	0.1320	38.3716
0.500	1.8137	0.297	0.2188	87.2036
1.000	3.6207	0.452	0.3375	174.4053
2.000	7.2380	0.696	0.5238	348.8093
5.000	18.0925	1.248	0.9458	872.0229
10.000	36.1844	1.951	1.4870	1744.0461
15.000	54.2764	2.535	1.9407	2616.0693
22.000	79.6054	3.246	2.4978	3836.8989
50.000	180.9214	5.493	4.2994	8720.2266
75.000	271.3823	7.127	5.6256	---
100.000	361.8430	8.627	6.8094	---
150.000	542.7634	11.129	8.9150	---
175.000	633.2231	12.330	9.8773	---
200.000	723.6838	13.474	10.7948	---
225.000	814.1440	14.572	11.6748	---
250.000	904.6057	15.63C	12.5228	---

The results of numerical evaluations of Eqs.(4.20), (4.21) ,(4.22) and (4.23) are listed in the Table II. The plots for above equations are shown in Figure 4.5.

For comparison, the crossing frequencies with von Karman spectral expression for the x and z directions are plotted in Figure 4.6. The crossing frequency for the z direction is less than the x direction except ideal band-pass filter case, in which the frequencies are identical for both directions.

The crossing frequency plots presented in Figures 4.4 - 4.6 offer a detailed view of how the crossing frequency depends on the filter function. Thus, in designing a system, the type of the filter has to be chosen carefully to match the behavior of the particular system.

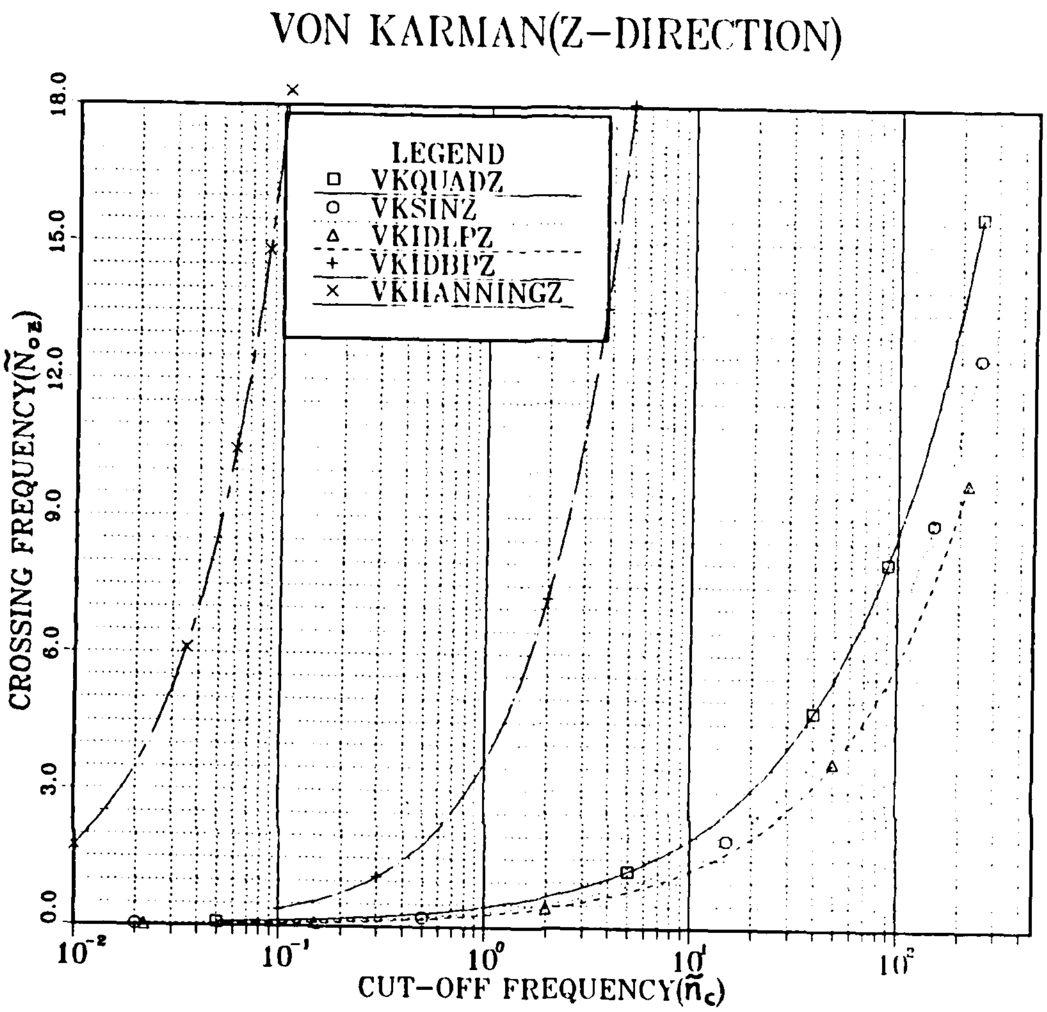

Figure 4.5 Crossing Frequencies with von Karman Spectral Expression for the z-direction.

2. Using the Kaimal Spectral Density Function

From Equation (3.4), the asymptotic spectral behavior can be written as

$$\frac{nS_i(n)}{\sigma_i^2} = \begin{cases} (f/f_o)^{-2/3} & ;\ f \gg f_o \quad (4.24a) \\ 0.164(f/f_o) & ;\ f \ll f_o \quad (4.24b) \end{cases}$$

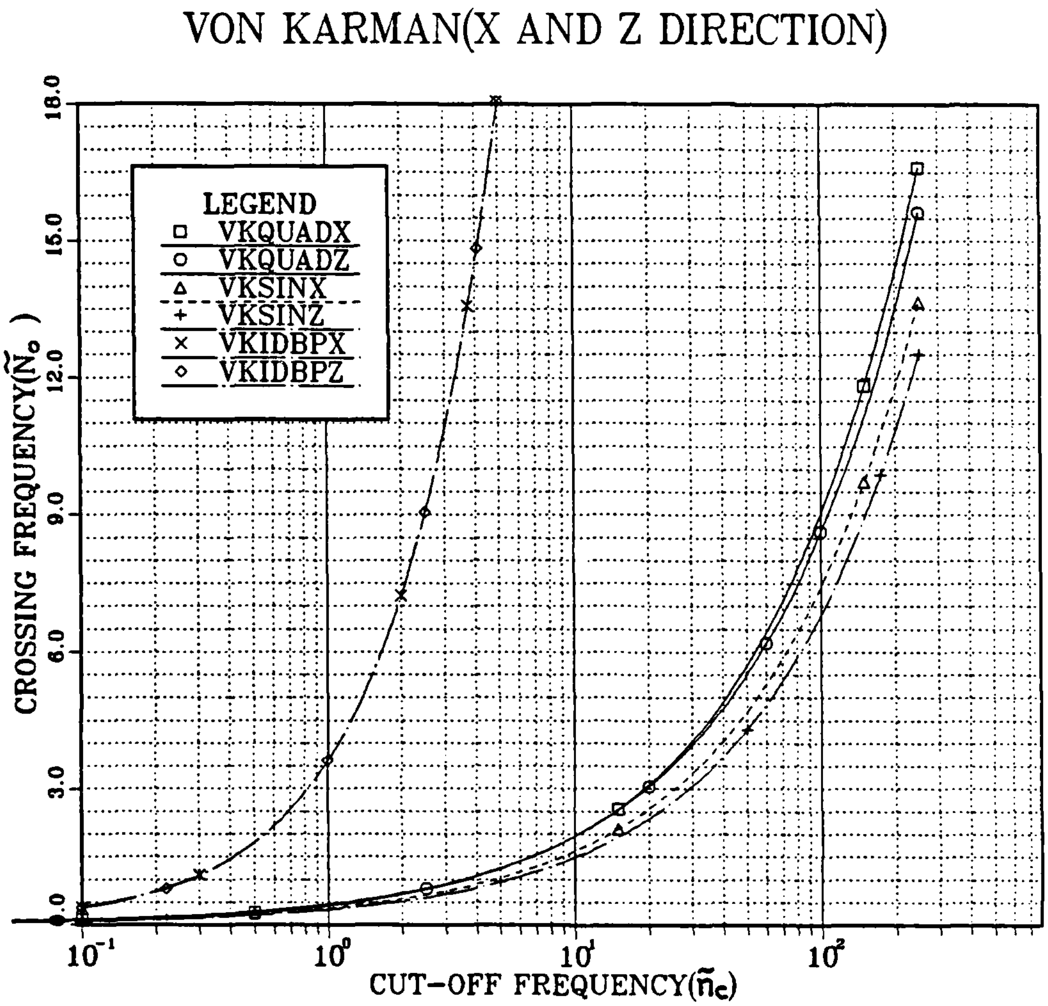

Figure 4.6 Crossing Frequencies with von Karman Spectral Expression for the x and z-direction.

The expression for the low frequency behavior of the spectrum is given

$$\frac{nS_i(n)}{\sigma_i^2} = (4L_i/z)f \tag{4.25}$$

where L_i represents the length scale. Equating Equation (4.25) and Equation (4.24b) becomes

$$L_i = 0.041z/(f_o)_\alpha \tag{4.26}$$

For the x-direction only

$$L_u = 0.041z/f_{ox}$$

or
$$f_{ox} = 0.041z/L_u \tag{4.27}$$

Substituting Equation(4.27) into (3.4) yields

$$\frac{nS_u(n)}{\sigma_u^2} = \frac{0.164(f/0.041z/L_u)}{1+0.164(f/0.041z/L_u)}$$

or
$$\frac{nS_u(n)}{\sigma_u^2} = \frac{4\tilde{n}}{1+33.641\tilde{n}^{5/3}} \tag{4.28}$$

where $\tilde{n} = nL_u/U$. Then the crossing frequency for the X-direction becomes

$$\tilde{N}_{ox} = \left[\int_0^\infty \frac{F(n)\,n^2\,dn}{(1+33.641\tilde{n}^{5/3})} \Bigg/ \int_0^\infty \frac{F(n)\,dn}{(1+33.641\tilde{n}^{5/3})}\right]^{1/2} \tag{4.29}$$

Substituting the quadratic filter function into Equation(4.29) yields

$$\tilde{N}_{ox} = \left[\frac{\displaystyle\int_0^\infty \frac{n^2\,dn}{(1+33.641\tilde{n}^{5/3})\,(n_c^2+n^2)}}{\displaystyle\int_0^\infty \frac{dn}{(1+33.641\tilde{n}^{5/3})\,(n_c^2+n^2)}}\right]^{1/2} \tag{4.30}$$

Replacing n/n_c by y in Equation(4.30) leads to

$$\tilde{N}_{ox} = \tilde{n}_c\left\{\frac{\displaystyle\int_0^\infty \frac{y^2\,dy}{[1+33.641(\tilde{n}_c\,y)^{5/3}](1+y^2)}}{\displaystyle\int_0^\infty \frac{dy}{[1+33.641(\tilde{n}_c\,y)^{5/3}](1+y^2)}}\right\}^{1/2} \tag{4.31}$$

Setting $y=e^{x}$ in Equation (4.31) gives

$$\tilde{N}_{ox} = \tilde{n}_c \left\{ \frac{\int_0^\infty \frac{e^{3x}\,dx}{[1+33.641(\tilde{n}_c e^x)^{5/3}](1+e^{2x})}}{\int_0^\infty \frac{e^{x}\,dx}{[1+33.641(\tilde{n}_c e^x)^{5/3}](1+e^{2x})}} \right\}^{1/2} \tag{4.32}$$

If we introduce the sine filter function into Equation (4.29), the crossing frequency becomes

$$N_{ox} = \left[\frac{\int_0^\infty \frac{\sin^2(0.44\pi n/n_c)\, n^2\, dn}{(1+33.641\tilde{n}^{5/3})\,(0.44\pi/n_c)^2\, n^2}}{\int_0^\infty \frac{\sin^2(0.44\pi n/n_c)\, dn}{(1+33.641\tilde{n}^{5/3})\,(0.44\pi/n_c)^2\, n^2}} \right]^{1/2} \tag{4.33}$$

Substituting $0.44\pi n/n_c$ for y in Equation (4.33), and define $\tilde{n}_c/0.44\pi=\tilde{\eta}_c$, yields

$$\tilde{N}_{ox} = \tilde{\eta}_c \left[\frac{\int_0^\infty \frac{\sin^2(y)\,dy}{1+33.641(\tilde{\eta}_c y)^{5/3}}}{\int_0^\infty \frac{[\sin^2(y)/y^2]\,dy}{1+33.641(\tilde{\eta}_c y)^{5/3}}} \right]^{1/2} \tag{4.34}$$

For the Hanning filter, substituting Equation (4.18) into Equation (4.28), setting $y=0.375\pi n/n_c$ and define $\tilde{n}_c/0.375\pi=\tilde{\eta}_c$, yields

$$\tilde{N}_{ox} = \tilde{\eta}_c \left\{ \frac{\displaystyle\int_0^\infty \frac{\sin^2(y)\,dy}{[1+33.641(\tilde{\eta}_c y)^{5/3}]\;(\pi^2-y^2)^2}}{\displaystyle\int_0^\infty \frac{[\sin^2(y)/y^2]\,dy}{[1+33.641(\tilde{\eta}_c y)^{5/3}]\;(\pi^2-y^2)^2}} \right\}^{1/2} \tag{4.35}$$

TABLE III

Crossing Frequencies (Kaimal x-direction)

$\tilde{n}_c$	IDBP	QUAD	SINE	HANNING
0.100	0.4056	0.134	0.0868	17.4532
0.125	0.4938	0.152	0.1001	21.8126
0.150	0.5819	0.169	0.1126	26.1720
0.175	0.6702	0.184	0.1243	30.5316
0.220	0.8295	0.210	0.1441	38.3790
0.500	1.8305	0.340	0.2445	87.2088
1.000	3.6321	0.518	0.3811	174.4094
2.000	7.2456	0.799	0.5943	348.8120
5.000	18.0968	1.434	1.0744	872.0224
10.000	36.1872	2.249	1.6879	1744.0486
15.000	54.2786	2.931	2.1987	2616.0667
22.000	79.6070	3.769	2.8249	3836.9033
50.000	180.9221	6.471	4.8291	8720.2461
75.000	271.3823	8.464	6.2923	---
100.000	361.8423	10.243	7.5860	---
150.000	542.7634	13.324	9.8619	---
175.000	633.2239	14.733	10.8962	---
200.000	723.6846	16.102	11.9076	---
225.000	814.1450	17.414	12.8333	---
250.000	904.6052	18.678	13.7017	---

The results of numerical calculations of Eqs. (4.29), (4.32), (4.34) and (4.35) are given in Table III and the plots for above equations are shown in Figure 4.7.

It is clear from the Eq. (3.4) and Eq. (4.26) that, for the Kaimal spectral density function, the difference in crossing frequencies between the x and z directions is only in the length scale L_i. Thus the plots for the z-direction are exactly same as the x-direction.

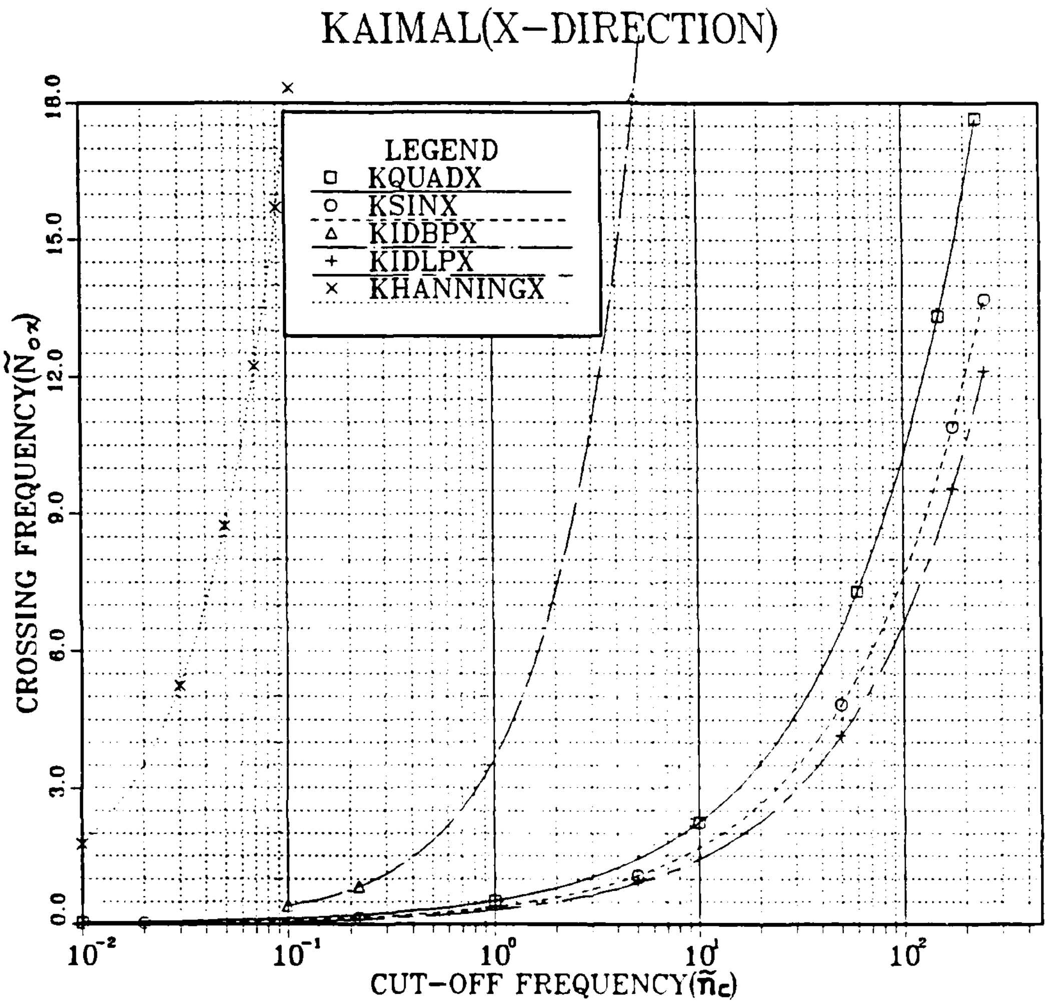

Figure 4.7 Crossing Frequencies with Kaimal Spectral Expression for the x-direction.

3. <u>Using the Teunissen Spectral Density Function</u>

The modified Kaimal spectral density expressions, which were derived by Teunissen, are given in Eqs. (3.5), (3.6) and (3.7). These equations were derived by adding a scaling parameter to each of the Kaimal spectral equations and evaluating these parameters from the observed data. These equations are function of friction velocity u_*. In

order to estimate the crossing frequency as we have done earlier, we need to change that equations as a function of variance. In E.S.D.U. [Ref. 5], the relations between σ_i and u_* are defined as

$$0.4\sigma_i/u_* = (\sigma_i/U)\log(\tilde{z}/z_o) \tag{4.36}$$

Teunissen derived the average values of σ_i/u_*, given by

$$\sigma_u/u_* = 2.84 \tag{4.37a}$$

$$\sigma_v/u_* = 1.92 \tag{4.37b}$$

$$\sigma_w/u_* = 1.27 \tag{4.37c}$$

From Equation(4.36) and Equation(4.37), one can get

$$u_*^2 \text{ (u-component)} = 0.124\ \sigma_u^2 \tag{4.38a}$$

$$u_*^2 \text{ (v-component)} = 0.271\ \sigma_v^2 \tag{4.38b}$$

$$u_*^2 \text{ (w-component)} = 0.620\ \sigma_w^2 \tag{4.38c}$$

and substituting Eq.(4.38) into Eqs.(3.5), (3.6) and (3.7) yields

$$\frac{nS_u(n)}{\sigma_u^2} = \frac{13\tilde{n}}{(0.44+33\tilde{n})^{5/3}} \tag{4.39}$$

$$\frac{nS_v(n)}{\sigma_v^2} = \frac{4.61\tilde{n}}{(0.38+9.5\tilde{n})^{5/3}} \tag{4.40}$$

$$\frac{nS_w(n)}{\sigma_w^2} = \frac{1.24\tilde{n}}{0.44+5.3\tilde{n}^{5/3}} \tag{4.41}$$

Using methods similar to the above, the crossing frequency for the x-direction, with the ideal band pass filter, becomes

As a consequence of the results studied herein, it is suggested that, in future work, careful consideration should be given to the type of filtering used to model structural behavior and determine more accurately the fatigue life of a system.

V. CONCLUSIONS

This study has estimated the crossing frequency based on the three spectral density functions, which assumes turbulence to be a homogeneous, stationary Gaussian process, with five different filter functions for the x and z directions.

This estimation has shown, for the x direction, that the Kaimal spectral function gives about one percent higher crossing frequency than the von Karman, and forty percent higher than the Teunissen one, at $\tilde{n}_c$=100 for quadratic-type filtering; for the ideal low-pass and sine-type filters, the difference between the Kaimal and von Karman spectral function is only a few percent, but for the Teunissen one is more than forty percent than for the other spectrums.

For the z direction, the Teunissen spectral function gives about ten percent higher crossing frequency than the Kaimal one and about twenty percent higher than the von Karman one, at $\tilde{n}_c$=100 for the quadratic-type, sine-type and low-pass filtering. However, this difference becomes to zero as non-dimensional cut-off frequency goes to zero.

The crossing frequencies for band-pass and Hanning filtering are only a fraction of a percent different for the three spectral functions.

The present study shows that Hanning and band-pass filtering predicts higher crossing frequencies than low-pass filtering. This difference is greatly amplified with the higher frequency.

If some site statistics are available, as for the example calculation, then the number of crossings that the wind-speed fluctuations exceed their zero value per a certain period can be computed and an estimation of fatigue life can be obtained.

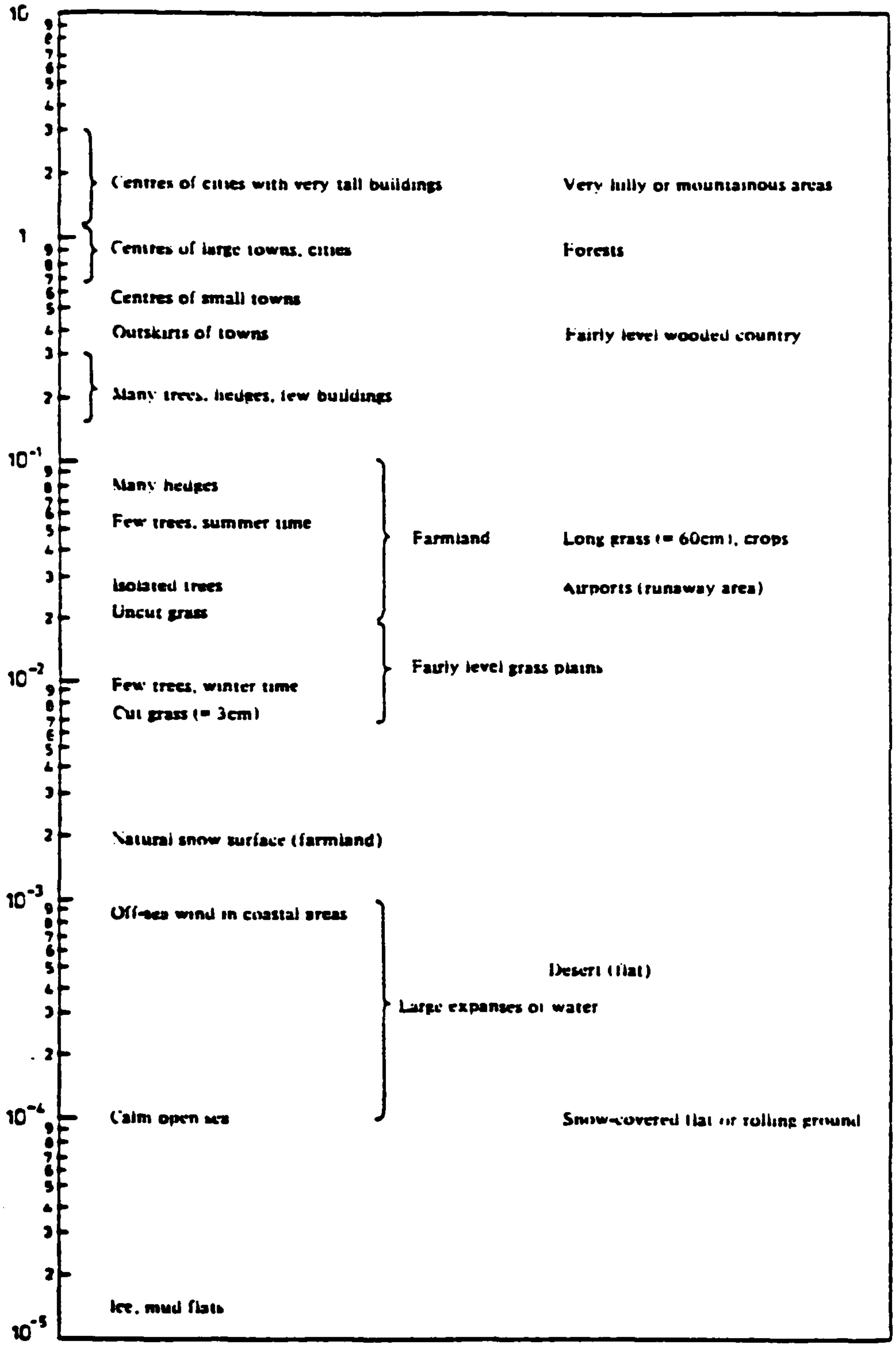

Figure 4.13 Values of the Surface Roughness Parameter z_0 (Reproduced from ESDU 74031).

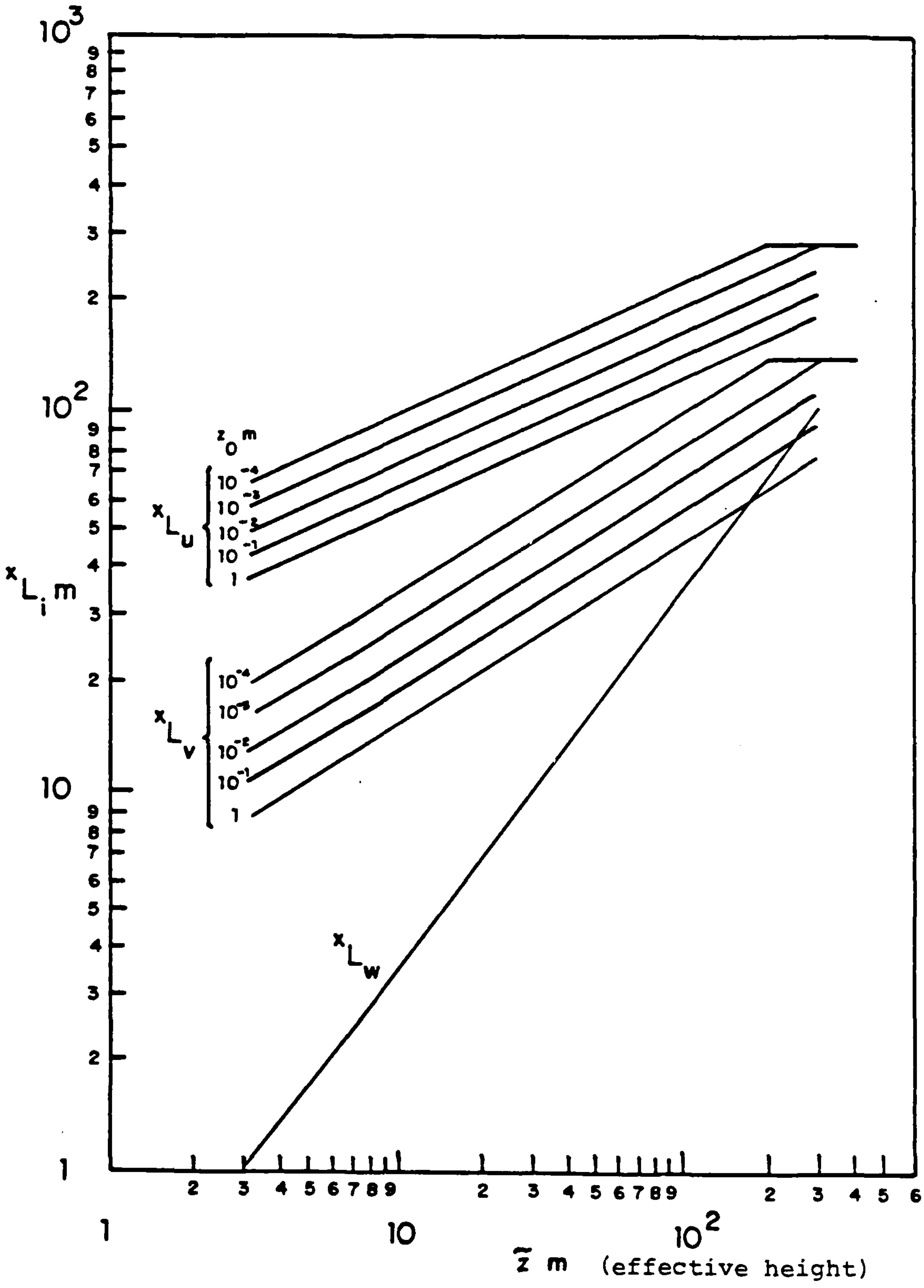

Figure 4.12 Values of Length Scale Parameter L_i (Reproduced from ESDU 74031).

TABLE VI

Example Calculations of the Crossing Frequency

von Karman (x-direction)

REMARK	IDBP	IDLP	QUAD	SINE
$\tilde{N}ox$	75.0	10.2	14.6	12.0
Nox	17.857	2.428	3.476	2.857

($\tilde{n}_{cu}$=210.0, U/Lu=0.238)

von Karman (z-direction)

REMARK	IDBP	IDLP	QUAD	SINE
$\tilde{N}oz$	4.70	1.50	2.40	1.80
Noz	18.076	5.769	9.231	6.923

($\tilde{n}_{cw}$=13, U/Lw=3.846)

Kaimal (x and z-direction)

REMARK	IDBP	IDLP	QUAD	SINE
$\tilde{N}ox$	75.0	10.9	16.50	12.2
Nox	17.857	2.595	3.928	2.905
$\tilde{N}oz$	4.70	1.70	2.65	2.05
Noz	18.076	6.538	10.192	7.885

Teunissen (x and z-direction)

REMARK	IDBP	IDLP	QUAD	SINE
$\tilde{N}ox$	75.0	6.08	9.30	6.50
Nox	17.857	1.448	2.214	1.548
$\tilde{N}oz$	4.70	2.10	3.30	2.40
Noz	18.076	8.076	12.692	9.230

z_o=0.001. The length scale parameters are given in Figure 4.12, and are given as L_u=105, L_v=36 and L_w=6.5.

The next step is calculation of the dimensionless cut-off frequencies, i.e.,

$$\tilde{n}_{cu} = nL_u/U = 210 \qquad (4.50)$$
$$\tilde{n}_{cv} = nL_v/U = 72$$
$$\tilde{n}_{cw} = nL_w/U = 13$$

The crossing frequencies are calculated by the use of the given crossing frequency vs cut-off frequency graphs, with dimensionless cut-off frequencies which are given in Eq.(4.50).

The final step is to convert the dimensionless crossing frequency to a dimensional frequency by multiplying the factor U/L_i, i.e.,

$$N_{ox} = \tilde{N}_{ox}\, U/L_u \qquad (4.51)$$
$$N_{oz} = \tilde{N}_{oz}\, U/L_w$$

The results of calculation of the crossing frequency for a given turbulence condition are given in Table VI.

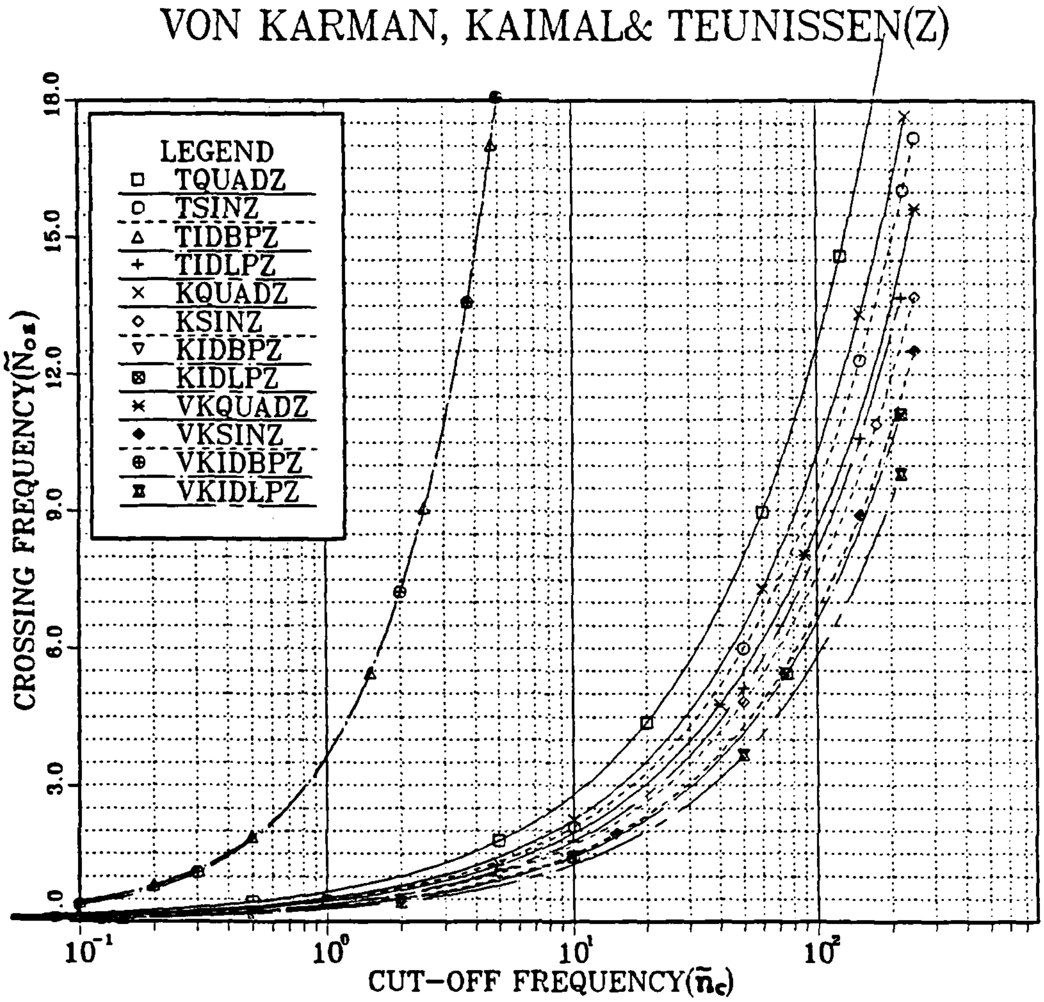

Figure 4.11 Comparison of von Karman, Kaimal and Teunissen Spectral Density Function for the z-direction.

Suppose we have a site for which

$\tilde{z}$ = 20m

n_c = 50Hz

U = 25m/sec and the turbulence condition is that for an off-sea wind in a coastal area.

With this choice of turbulence condition, the surface roughness parameter z_o can be found in Figure 4.13, and is

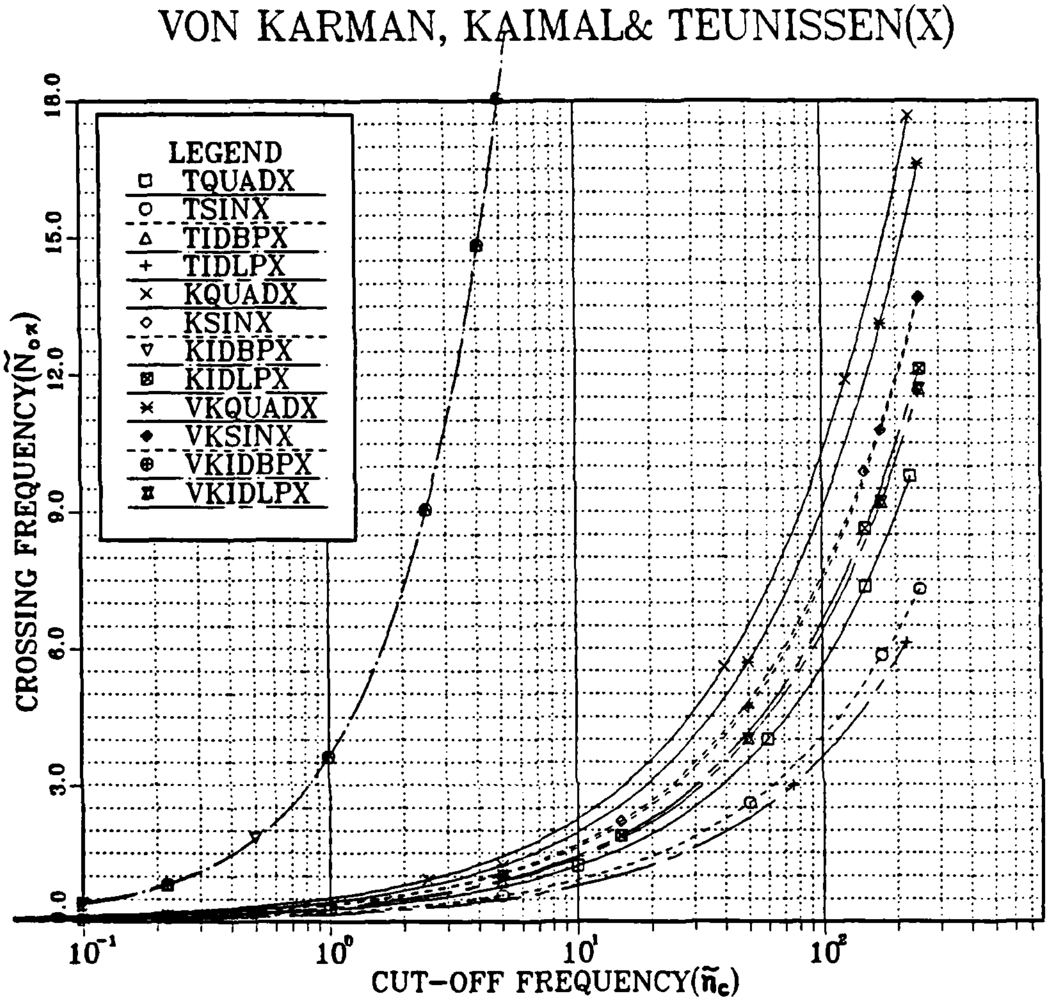

Figure 4.10 Comparison of von Karman, Kaimal and Teunissen Spectral Density Function for the x-direction.

The dimensionless crossing frequency, $\tilde{N}_{oi}$, is a function of $\tilde{n}_c$ $(=nL_i\ /U)$. The length scale parameter L_i and surface roughness parameter z_o are given by E.S.D.U. [Ref. 5]. For convenience these data are included here as Figure 4.12 for length scale parameters, and Figure 4.13 for the surface roughness parameters.

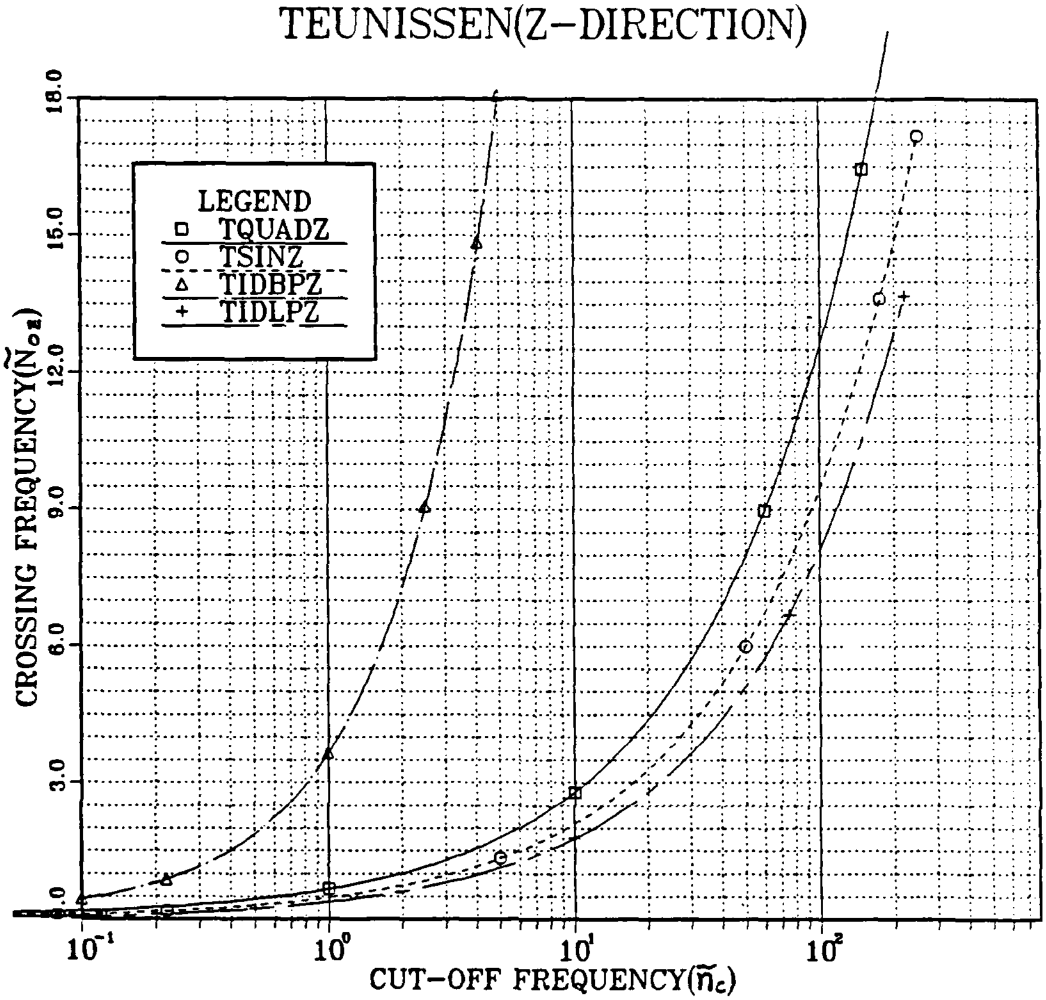

Figure 4.9 Crossing Frequencies with Teunissen Spectral Density Function for the z-direction.

C. EXAMPLE CALCULATIONS

In the previous section of this study, we derived equations for the crossing frequency. The purpose of this section is to illustrate the application of these equations to a given turbulence condition, and to estimate the crossing frequencies for a low-pass filter.

TABLE V

Crossing Frequencies (Teunissen z-direction)

$\tilde{n}_c$	IDBP	QUAD	SINE	IDLP
0.100	0.4454	0.178	0.1098	0.0559
0.125	0.5367	0.201	0.1258	0.0691
0.150	0.6263	0.222	0.1408	0.0818
0.175	0.7151	0.241	0.1551	0.0941
0.220	0.8740	0.274	0.1794	0.1153
0.500	1.8651	0.438	0.3047	0.2268
1.000	3.6560	0.660	0.4758	0.3783
2.000	7.2610	1.007	0.7414	0.6104
5.000	18.1053	1.789	1.3353	1.1232
10.000	36.1926	2.791	2.0917	1.7725
15.000	54.2827	3.629	2.7242	2.3144
22.000	79.6102	4.658	3.5000	2.9785
50.000	180.9239	7.973	5.9955	5.1216
75.000	271.3835	10.410	7.8197	6.6982
100.000	361.8437	12.591	9.4420	8.1050
150.000	542.7644	16.470	12.3095	10.6064
175.000	633.2249	18.242	13.6158	11.7493
200.000	723.6853	19.932	14.8606	12.8388
225.000	814.1458	21.553	16.0474	13.8837
250.000	904.6062	23.115	17.1816	14.8905

For comparison, the crossing frequencies with the von Karman, Kaimal and Teunissen spectral expressions for the x-direction with various filter functions are plotted in Figure 4.10. As shown in Figure 4.10, the crossing frequencies predicted by the Kaimal spectral expression are higher than for the others. In Figure 4.11, the crossing frequencies, with all three spectral expressions and the z-direction, are compared. The figure characteristics are similar to those for the x-direction, except that the crossing frequencies are lower.

If one introduces the sine filter function, the equation for the crossing frequency becomes

$$N_{oz} = \left[\frac{\displaystyle\int_0^\infty \frac{\sin^2(0.44\pi n/n_c)\, n^2\, dn}{(0.44+5.3\tilde{n}^{5/3})\,(0.44\pi n/n_c)^2}}{\displaystyle\int_0^\infty \frac{\sin^2(0.44\pi n/n_c)\, dn}{(0.44+5.3\tilde{n}^{5/3})\,(0.44\pi n/n_c)^2}} \right]^{1/2} \qquad (4.47)$$

or

$$\tilde{N}_{oz} = \tilde{\eta}_c \left\{ \frac{\displaystyle\int_0^\infty \frac{\sin^2(y)\, dy}{0.44+5.3(\tilde{\eta}_c y)^{5/3}}}{\displaystyle\int_0^\infty \frac{[\sin^2(y)/y^2]\, dy}{0.44+5.3(\tilde{\eta}_c y)^{5/3}}} \right\}^{1/2} \qquad (4.48)$$

If one introduces the quadratic filter function, the equation for the crossing frequency becomes

$$\tilde{N}_{oz} = \tilde{n}_c \left\{ \frac{\displaystyle\int_0^\infty \frac{y^2\, dy}{[0.44+5.3(\tilde{n}_c y)^{5/3}]\,(1+y^2)}}{\displaystyle\int_0^\infty \frac{dy}{[0.44+5.3(\tilde{n}_c y)^{5/3}]\,(1+y^2)}} \right\}^{1/2} \qquad (4.49)$$

The results of numerical calculations of Eqs. (4.46), (4.48) and (4.49) are given in Table V. The plots for above equations are shown in Figure 4.9.

or

$$\tilde{N}_{oz} = \tilde{n}_{c1}\left[\int_{n_{c1}}^{n_{c2}} \frac{y^2\,dy}{0.44+5.3(\tilde{n}_{c1}\,y)^{5/3}} \Bigg/ \int_{n_{c1}}^{n_{c2}} \frac{dy}{0.44+5.3(\tilde{n}_{c1}\,y)^{5/3}}\right]^{1/2} \quad (4.46)$$

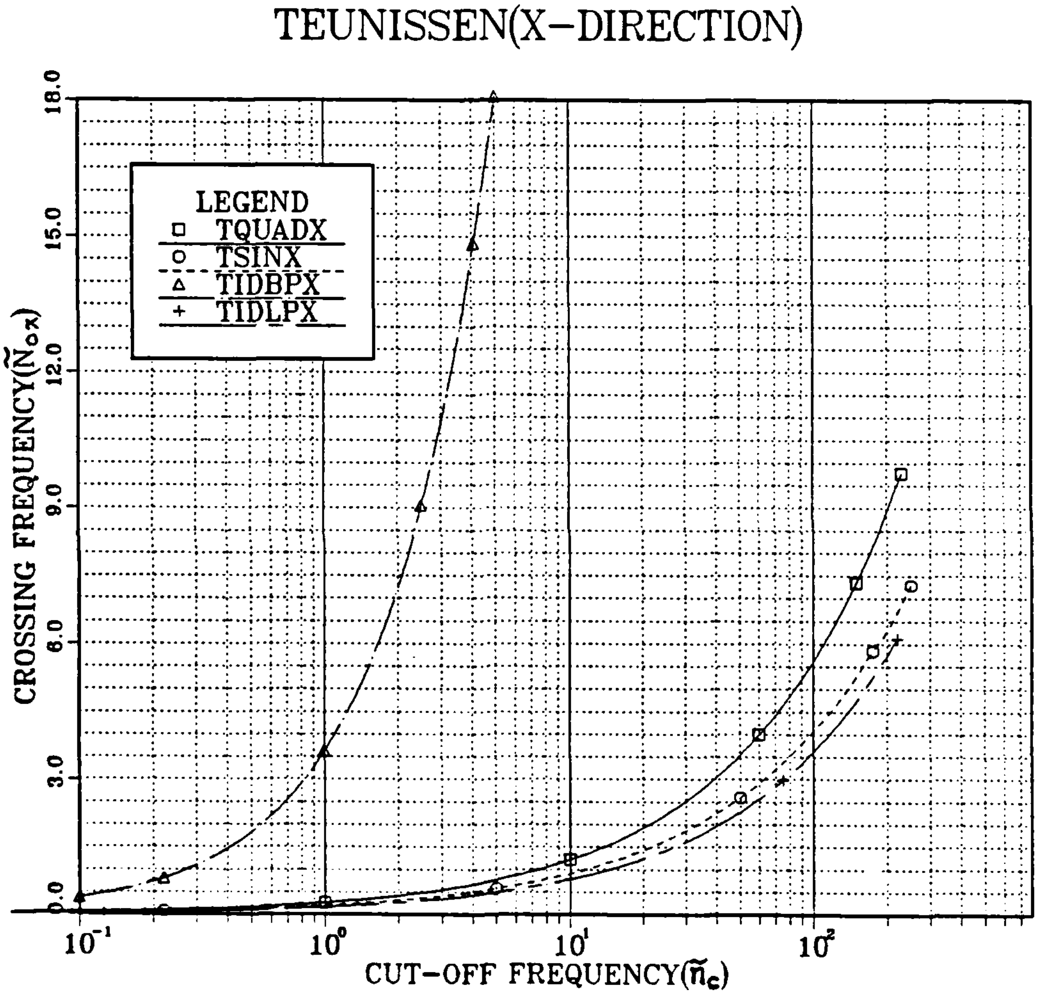

Figure 4.8 Crossing Frequencies using Teunissen Spectral Expression for the x-direction.

TABLE IV

Crossing Frequencies (Teunissen x-direction)

$\tilde{n}_c$	IDBP	QUAD	SINE	IDLP
0.100	0.3722	0.060	0.0425	0.0334
0.125	0.4628	0.069	0.0494	0.0394
0.150	0.5534	0.078	0.0559	0.0449
0.175	0.6439	0.086	0.0620	0.0502
0.220	0.8068	0.099	0.0724	0.0590
0.500	1.8201	0.169	0.1251	0.1044
1.000	3.6294	0.266	0.1983	0.1672
2.000	7.2478	0.420	0.3142	0.2664
5.000	18.1031	0.768	0.5754	0.4915
10.000	36.1952	1.213	0.9083	0.7801
15.000	54.2873	1.581	1.1846	1.0219
22.000	79.6162	2.039	1.5228	1.3188
50.000	180.9321	3.521	2.6002	2.2786
75.000	271.3931	4.612	3.3801	2.9851
100.000	361.8535	5.586	4.0689	3.6157
150.000	542.7749	7.266	5.2816	4.7372
175.000	633.2354	8.053	5.8554	5.2496
200.000	723.6956	8.804	6.2870	5.7380
225.000	814.1565	9.525	6.8032	6.2065
250.000	904.6169	10.219	7.3011	6.6579

The results of numerical calculations of Eqs. (4.42), (4.44) and (4.45) are given in Table IV and the plots for these equations are shown in Figure 4.8.

The modified Kaimal spectral expression for the z-direction is given by Eq. (4.41). If we put ideal band pass filter function and spectral expression for the z-directon into Eq. (4.2) it yields

$$N_{oz} = \left[\int_{n_{c1}}^{n_{c2}} \frac{n\, dn}{0.44+5.3\tilde{n}^{5/3}} \Big/ \int_{n_{c1}}^{n_{c2}} \frac{dn}{0.44+5.3\tilde{n}^{5/3}} \right]^{1/2}$$

$$N_{ox} = \left[\int_{n_{c1}}^{n_{c2}} \frac{n^2 dn}{(0.44+33\tilde{n})^{5/3}} \Big/ \int_{n_{c1}}^{n_{c2}} \frac{dn}{(0.44+33n)^{5/3}} \right]^{1/2}$$

or $$\tilde{N}_{ox} = \tilde{n}_{c1} \left[\int_{n_{c1}}^{n_{c2}} \frac{y^2 dy}{(0.44+33\tilde{n}_{c1}\, y)^{5/3}} \Big/ \int_{n_{c1}}^{n_{c2}} \frac{dy}{(0.44+33\tilde{n}_{c1}\, y)^{5/3}} \right]^{1/2} \quad (4.42)$$

If one uses the sine filter function, with cut-off frequency n_c=0.44/T, the crossing frequency becomes

$$N_{ox} = \left[\frac{\displaystyle\int_0^{\infty} \frac{\sin^2(0.44\pi n/n_c)\, n^2\, dn}{(0.44+33\tilde{n})^{5/3}\ (0.44\pi n/n_c)^2}}{\displaystyle\int_0^{\infty} \frac{\sin^2(0.44\pi n/n_c)\, dn}{(0.44+33\tilde{n})^{5/3}\ (0.44\pi n/n_c)^2}} \right]^{1/2} \quad (4.43)$$

Setting $y=0.44\pi n/n_c$ into Eq. (4.43), and define $\tilde{n}_c/0.44\pi=\tilde{\eta}_c$, yields

$$\tilde{N}_{ox} = \tilde{\eta}_c \left\{ \int_0^{\infty} \frac{\sin^2(y)\, dy}{(0.44+33\tilde{\eta}_c\, y)^{5/3}} \Big/ \int_0^{\infty} \frac{[\sin^2(y)/y^2]\, dy}{(0.44+33\tilde{\eta}_c\, y)^{5/3}} \right\}^{1/2} \quad (4.44)$$

For the quadratic filter function, $\tilde{N}_{ox}$ becomes

$$\tilde{N}_{ox} = \tilde{n}_c \left[\frac{\displaystyle\int_0^{\infty} \frac{y^2 dy}{(0.44+33\tilde{n}_c\, y)^{5/3}\ (1+y^2)}}{\displaystyle\int_0^{\infty} \frac{dy}{(0.44+33\tilde{n}_c\, y)^{5/3}\ (1+y^2)}} \right]^{1/2} \quad (4.45)$$

LIST OF REFERENCES

1. Dryden, H.L., "A Review of the Statistical Theory of Turbulence," Turbulence Classic Paper on Statistical Theory, New York, Interstate Publishers,Inc., 1961.

2. von Karman, T., and Howarth, L., "On the Statistical Theory of Isotropic Turbulence," Proceedings, Royal Society of London, Series A, 164, 1938.

3. Kaimal, J.C., "Turbulence Spectra, Length Scales and Structure Parameters in the Stable Surface Layers", Boundary-Layer Meteorology, vol. 4, pp. 289-309, 1973.

4. Teunissen, H.W., "Structure of Mean Winds and Turbulence in the Planetary Boundary Layer over Rural Terrain", Boundary-Layer Meteorology, vol. 2, pp. 187-221, September 1980.

5. "Characteristics of Atmospheric Turbulence Near the Ground", Engineering Sciences Data Unit, Part2, Item 74031, 1974.

6. Powell, D.C. and Connell, J.R., Definition of Gust Model Concepts and Review of Gust Models, PNL-3138, Pacific Northwest Laboratory, Richmond, Washington, June 1980.

7. Dutton, J.A., "Broadening Horizons in Prediction of the Effects of Atmospher Turbulence on Aeronautical Systems," AIAA 5th Annual Meeting and Technical Display, Paper No. AIAA-68-1065, 1968.

8. Jones, J.W., and others, Low Altitude Atmospheric Turbulence LO-LOCAT Phase3, Airforce Flight Dynamic Lab. Technical Report, AFFDL-TR-70-10, 1970.

9. Reeves, R.M., Joppa, R.G. and Ganzer, V.M., A Non-Gaussian Model of Continuous Atmospheric Turbulence for Use in Aircraft Design, NASA CR-2639, January 1976.

10. Kaimal, J.C., Gaynor, J.E. and Wolfe, D.E., Turbulence Statistics for Design of Wind Turbine Generators, NOAA/ERL Wave Propagation Laboratory, Boulder, Colorado, December 1980.

11. Vinnichenko, N.E., and others, Turbulence in the Free Atmosphere, pp. 65-96, Consultants Bureau, New York, 1983.

12. Greenway, M.E., "AN Analytical Approach to Wind Velocity Gust Factors," Jounal of Industrial Aerodynamics, vol 5, pp. 61-91, 1979.

INITIAL DISTRIBUTION LIST

		No. Copies
1.	Defense Technical Information Center, Cameron Station, Alexandria, Virginia 22314	2
2.	Library, Code 0142 Naval Postgraduate School, Monterey, California 93943	2
3.	Department Chairman, Code 67 Department of Aeronautics, Naval Postgraduate School, Monterey, California 93943	2
4.	Professor J. V. Healey, Code 67He Department of Aeronautics, Naval Postgraduate School, Monterey, California 93943	1
5.	Professor R. W. Bell, Code 67Be Department of Aeronautics, Naval Postgraduate School, Monterey, California 93943	1
6.	Lee, Cheong Koo 434 Kwan-Joe Dong, Chung Ku, TaeJeon, Republic of Korea	2
7.	Song, Yeong Cheon 104-25 Doma-2dong, Chung Ku, TaeJeon, Republic of Korea	2

END

FILMED

6-85

DTIC